remote sensing

MDPI

Article

Rainfall Variability and Trends over the African Continent Using TAMSAT Data (1983–2020): Towards Climate Change Resilience and Adaptation

Niranga Alahacoon [1,2,*], Mahesh Edirisinghe [1], Matamyo Simwanda [3], ENC Perera [4], Vincent R. Nyirenda [5] and Manjula Ranagalage [6]

1 Department of Physics, University of Colombo, Colombo 00300, Sri Lanka; mahesh@phys.cmb.ac.lk
2 International Water Management Institute (IWMI), 127, Sunil Mawatha, Pelawatte, Batteramulla, Colombo 10120, Sri Lanka
3 Department of Plant and Environmental Sciences, School of Natural Resources, Copperbelt University, P.O. Box 21692, Kitwe 10101, Zambia; matamyo@gmail.com
4 Department of Regional Science and Planning, SANASA Campus, Kegalle 71000, Sri Lanka; chinssu@gmail.com
5 Department of Zoology and Aquatic Sciences, School of Natural Resources, Copperbelt University, P.O. Box 21692, Kitwe 10101, Zambia; vrnyirenda@hotmail.com
6 Department of Environmental Management, Faculty of Social Sciences and Humanities, Rajarata University of Sri Lanka, Mihintale 50300, Sri Lanka; manjularanagalage@gmail.com
* Correspondence: n.alahacoon@cgiar.org

Abstract: This study reveals rainfall variability and trends in the African continent using TAMSAT data from 1983 to 2020. In the study, a Mann–Kendall (MK) test and Sen's slope estimator were used to analyze rainfall trends and their magnitude, respectively, under monthly, seasonal, and annual timeframes as an indication of climate change using different natural and geographical contexts (i.e., sub-regions, climate zones, major river basins, and countries). The study finds that the highest annual rainfall trends were recorded in Rwanda (11.97 mm/year), the Gulf of Guinea (river basin 8.71 mm/year), the tropical rainforest climate zone (8.21 mm/year), and the Central African region (6.84 mm/year), while Mozambique (−0.437 mm/year), the subtropical northern desert (0.80 mm/year), the west coast river basin of South Africa (−0.360 mm/year), and the Northern Africa region (1.07 mm/year) show the lowest annual rainfall trends. There is a statistically significant increase in the rainfall in the countries of Africa's northern and central regions, while there is no statistically significant change in the countries of the southern and eastern regions. In terms of climate zones, in the tropical northern desert climates, tropical northern peninsulas, and tropical grasslands, there is a significant increase in rainfall over the entire timeframe of the month, season, and year. This implies that increased rainfall will have a positive effect on the food security of the countries in those climatic zones. Since a large percentage of Africa's agriculture is based only on rainfall (i.e., rain-fed agriculture), increasing trends in rainfall can assist climate resilience and adaptation, while declining rainfall trends can badly affect it. This information can be crucial for decision-makers concerned with effective crop planning and water resource management. The rainfall variability and trend analysis of this study provide important information to decision-makers that need to effectively mitigate drought and flood risk.

Keywords: rainfall variability; rainfall trend; TAMSAT data; climate change; climate hazard; Africa

Citation: Alahacoon, N.; Edirisinghe, M.; Simwanda, M.; Perera, E.; Nyirenda, V.R.; Ranagalage, M. Rainfall Variability and Trends over the African Continent Using TAMSAT Data (1983–2020): Towards Climate Change Resilience and Adaptation. *Remote Sens.* **2022**, *14*, 96. https://doi.org/10.3390/rs14010096

Academic Editor: Silas Michaelides

Received: 26 November 2021
Accepted: 23 December 2021
Published: 25 December 2021

Publisher's Note: MDPI stays neutral with regard to jurisdictional claims in published maps and institutional affiliations.

1. Introduction

There has been a clear change in the global climate in recent decades that could significantly impact environmental, social, and economic sustainability [1–3]. The changes in spatial and temporal variability of rainfall have been observed in various parts of the world [4]. In 2021, for example, almost all the continents experienced severe flooding

with both positive and negative impacts [5]. The unprecedented droughts accompanied by severe wildfires experienced between 2020 and 2021 across the United States, Brazil's Amazon rainforest, Australia, and Europe are an indication of the negative impacts of reducing rainfall [6–9]. Furthermore, the variability in rainfall can have a significant impact on ecosystems and their biodiversity, positively or negatively [10–12].

Climate variability directly impacts agriculture and poses a significant threat to food security and livelihoods, especially in poor or developing countries [13]. Many recent studies have shown an increase in rainfall over countries around the world and notably a decrease in rainfall over southern Africa [14–21]. Africa has been identified by various studies as increasingly vulnerable to climate change and variability, with one of the significant impacts being the reduction in agricultural production due to the continent's low adaptive capacity [20,22]. About 80% of the total human population in Africa is dependent on agriculture or agricultural products, while in most African countries, the fiscal contribution of the agricultural sector to GDP is more than 40% [23].

Rainfall and temperature are the major determinants of climate variability. A significant increase or decrease in rainfall can also be detected by long-term changes in the monsoon system [24,25]. However, Africa receives rainfall over two major monsoons: The West African monsoon (WAM) and the East African monsoon (EAM). During the WAM, winds blow southwest from the North Atlantic Ocean, keeping the Inter-Tropical Convergence Zone (ITCZ) above the equator, and WAM usually occurs from June to September [26,27]. West African Sahel became known as having the region's most devastating drought because of changes in WAM conditions during the 1970s and 1980s [28,29]. During the EAM seasons, the ITCZ is located south of the equator, with long-duration rain from March to May and short duration rain from October to December in the central, southern, and eastern parts of Africa [24,30].

In addition to the two major monsoon seasons, WAM and EAM, the IPCC Atlas (IPCC, 2013 [2]) introduced another four rainfall seasons, Mar–Apr–May (MAM), Jun–Jul–Aug (JJA), Sep–Oct–Nov (SON), and Dec–Jan–Feb (DJF) in order to study and compare the climate variability effectively across geographies. Moreover, various studies [31–34] have shown that the rainfall variability in Africa is more sensitive to large-scale climatic variables, such as "El Niño-Southern Oscillation (ENSO)", La Niña-Southern Oscillation (ENSO), Indian Ocean Depot (IOD), and ITCZ.

Rainfall variability and its trends are important for water resource management, climate variability assessment, and determining changes in its impacts on water resources [35,36]. The foremost obstacle to a detailed rainfall trend analysis using data measured from field-based meteorological stations covering the entire African continent is the unavailability of adequate long-term and spatially represented climatic data [20,37]. Station-based rainfall measurements for large areas are unavailable at high intensities with spatial frequencies [38], a situation that renders low-quality data. The rainfall trend studies conducted with high-quality data can form a basis to manage climate impacts better [39]. There have been several studies on long-term variability in rainfall parameters and trends covering mosaics of Africa, most of which are based on a particular region, river basin, country, or a region of a country [40,41]. The most commonly used climatic data for those studies are location-specific or climatic models with coarser spatial resolution. However, only a handful of studies have been conducted using satellite estimated rainfall data to derive the rainfall trends [42,43].

Rainfall estimates based on satellite or hybrid (satellite and ground data) provide a practical and complementary alternative to ground data in the absence of long-term field-measured rainfall data [20]. On the other hand, the use of high-resolution raster rainfall data, generated using either satellite estimates or models, is appropriate for a variety of analyses, including those of the rainfall trends and of the drought monitoring, by the capturing of spatial variability of a considered geographical area [44]. Satellite-based rainfall estimates have the advantage of providing full spatial coverage of the particular area, using a variety of algorithms [45–48]. The well-known major precipitation

products available globally and regionally that can be used successfully for the above approach are the Tropical Rainfall Measuring Mission (TRMM; [49]), Global Precipitation Climatology Center (GPCC; [50]), Asian Precipitation-Highly-Resolved Observational Data Integration Towards Evaluation (APHRODITE; [51]), Global Precipitation Measurement (GPM; [52]), Precipitation Estimation from Remotely Sensed Information using Artificial Neural Networks (PERSIANN; [53]), Climate Hazards Group InfraRed Precipitation with Stations data (CHIRPS; [54]), and Tropical Applications of Meteorology Using Satellite Data and Ground-Based Observations (TAMSAT; [42,44]).

Long-term rainfall variability and trend studies provide significant support for identifying areas with significant changes in rainfall patterns. However, such studies have not been undertaken in such a way as to cover the entire African continent, and if such studies had been conducted, they would have been more helpful to the development of policy-making and implementation processes in all fields. Besides, identifying continental-wide long-term rainfall variability and trends by considering spatial and temporal variability would greatly help agro-meteorologists and disaster management decision-makers and practitioners. It would further enhance African governments' capabilities in drought/flood monitoring, decision-making on crop diversification (i.e., essential strategy in food security), and infrastructure development, among several other applications. The rainfall variability is widely known to affect food security, with the worst scenario of reducing food availability and causing malnutrition [55]. Furthermore, rainfall variability can significantly increase hunger in countries with high rainfall variability, sensitive agriculture systems, and subsistence agriculture dependence for their livelihoods. Africa is most affected by rainfall variability, as rain-fed agriculture accounts for more than 90% of Africa's total agriculture [56–59].

Moreover, we contend that a study that covers the whole of Africa using a single dataset, such as TAMSAT, will provide a better overall rainfall distribution perspective, rather than identifying rainfall trends that cover small areas, especially using limited rainfall gauge data. When using a raster rainfall dataset that covers a large area at once, importantly, if data has some errors, it will distribute in the entire dataset evenly to minimize the impact of spatial outliers. Furthermore, rainfall trend studies covering the whole African continent are almost non-existent. This reflects the fact that studies in remote and data-deficient areas where much of the agricultural activities are limited, and as a result, areas in many parts of Africa are vulnerable to climate change and variability. Africa's rural areas are at greater risk of climate variability due to inadequate studies and information to develop strategies for risk management and climate resilience.

Intending to provide a successful solution to the aforementioned challenges, this study focuses on the African continent-wide analysis of long-term rainfall variability and trends based on TAMSAT data, using diverse geographical contexts (country, major river basins, regions, and climatic zones) and timeframes (monthly, seasonal and annual). Furthermore, this study investigates whether rainfall will vary significantly over time in different geographical units under the influence of different monsoons. A pathway to use rainfall variability and trends towards climate change resilience and adaptation is also discussed from multiple perspectives, such as agricultural crop diversification, water management, infrastructure development, and biodiversity conservation.

2. Materials and Methods

2.1. Study Area: African Continent

The African continent is located in the equatorial and subtropical latitudes of the Northern and Southern Hemispheres, having many different climatic conditions. Africa's climate includes tropical (desert, rainforest, grassland, and semi-arid) and subtropical (humid and desert) climate zones, as depicted in Figure 1a. It also experiences tropical monsoon seasons and consists of subtropical highlands. Africa is the largest tropical region among all continents of the Earth, and different vegetation is found in various ecosystems, including rainforests, tropical deserts, savannah, and grasslands [60]. As indicated in

Figure 1a, there are 25 major river basins in Africa, according to the United Nations' Food and Agriculture Organization [61]. Africa covers a total land area of 30.4 million square kilometres, 7500 km from north to south and 7300 km east-west covering 37°21′00″N–34°51′15″S, 17°31′13″W–51°27′52″E [62].

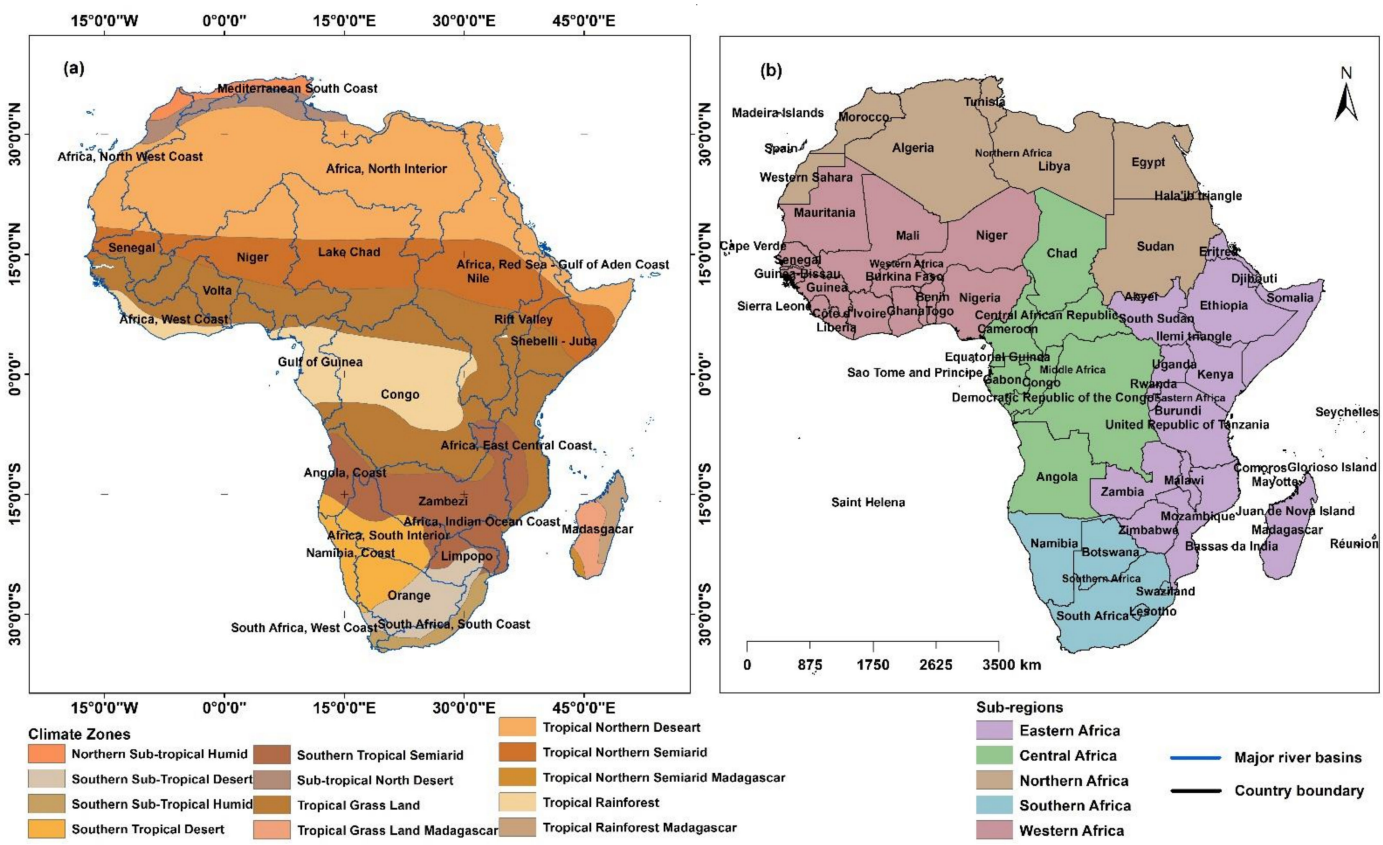

Figure 1. Study area: African continent. (**a**) climate zone and major river basins. (**b**) five regions and countries.

There are 68 countries in five sub-regions of the African continent (Figure 1b). The United Nations geoscheme (https://unstats.un.org/unsd/methodology/m49/, accessed on 4 April 2021), world atlas of Africa (https://www.worldatlas.com/geography/regions-of-africa.html, accessed on 4 June 2021) as well as the African Union (http://www.west-africa-brief.org/content/en/six-regions-african-union, accessed on 4 August 2021), have identified the five regions of Africa as Northern, Central (Middle), Western, Eastern, and Southern, with some changes of the number of countries in each region. The regional classification for the African continent, classified according to the United Nations geoscheme and World Atlas of Africa, was used for this study as most previous studies have also adapted the same African regions [63].

2.2. Data

Many studies have emphasized that rainfall products produced by the TAMSAT team at the University of Reading in the UK are more suitable than their surrogates for study in Africa, given the availability of the above rainfall estimates, TAMSAT's level of accuracy, its spatial resolution, and its widespread use for trend analysis [30,64–66]. The gridded TAMSAT rainfall products are based on high-resolution Meteosat thermal infrared (TIR) observations and data gathered through rainfall stations [67]. Furthermore, TAMSAT rainfall products provide a valuable basis for a more successful study of long-term rainfall trends as they are available from 1983 to the present, covering all of Africa at 4 km spatial resolution [43]. The TAMSAT data have been generated using the Meteosat data and

integrated ground data through an explorative calibration approach. Until 2009, TAMSAT data were only available for the Northern, Southern, and some parts of East African regions, but updated data from 1983 to date with calibrated measurement data entries for all of Africa are now available [42]. A systematic statistical assessment shows that the TAMSAT daily datasets are comparable to other remotely-sensed rainfall datasets and can be used for various applications with high accuracy. Although the suitability of TAMSAT data as aforestated, has been shown through various studies, in some instances overestimation and underestimation of rainfall can be identified. It might be due to the use of infrared data for TAMSAT rainfall estimates instead of Synthetic Aperture Radar (SAR) data [42]. Furthermore, the study by Ross (2016) concludes that TAMSAT data are well suited for risk assessments and long-term changes in rainfall. Henceforth, this study uses TAMSAT daily rainfall estimates from 1983 to 2020 as the main input rainfall data into our models.

African country and region boundaries were freely downloaded from the World Bank official boundary data catalogue (https://datacatalog.worldbank.org/dataset/world-bank-official-boundaries, accessed on 2 April 2021). The major river basins boundaries were downloaded from the FAO data catalogue (https://data.apps.fao.org/map/catalog/, accessed on 16 April 2021) considering its high accuracy. The main reason for that high accuracy is that the basin boundaries are extracted from hydrologically-corrected elevation data (WWF HydroSHEDS and Hydro1K). The climate zone map of Africa was generated using a raster dataset (https://www.britannica.com/place/Africa/Climate, accessed on 16 April 2021).

2.3. Methodology

2.3.1. Rainfall Data Pre-Processing

TAMSAT version 3.0 [41] daily rainfall data was downloaded from the University of Reading Research Data Archive from 1983 to 2020. Downloaded data are available as a single layer of NetCDF (Network Normal Data Format) file format 365 layers per year, with 13 880 layers for 38 years. These data layers were converted to a Tagged Image Format (.TIFF) using R-Studio software, as TIFF data could be handled more conveniently in the Geographical Information System (GIS).

Rainfall data for different periods of the month, season, and year were generated by aggregating daily TAMSAT data for the respective periods, and since this rainfall data can be obtained from the raster data format, the data accumulation process uses a geospatial data analysis method called cell statistics available in GIS. Since different geographical units, such as countries, river basins, regions, and meteorological zones, were used in this study, the average rainfall for each unit was calculated on monthly, seasonal, and annual bases. In order to calculate the spatial average of each geographic unit, the zonal average method was used. Subsequently, Mann–Kendall's test and Sen's slope estimate as defined below were used to analyze rainfall trends at different timeframes (i.e., monthly, seasonally, and annually) and geographical units (i.e., sub-regions, climate zones, major river basins, and countries).

2.3.2. Mann–Kendall's Trend Test

The Mann–Kendall (MK) non-parametric test was adopted in this study as it is commonly used to monitor the trends in inter alia, rainfall, temperature, and river discharge [68–70]. Positive values of the trend test's results indicate an increase in the parameters over time, while the negative values show a decreasing trend [71,72]. The trend analysis is performed in two stages, the first being the MK test, which examines whether there is a uniform linear increase or decrease tendency. Secondly, the slope of the linear trend created through the test is estimated using the non-parametric Sen's slope estimate, which gives a quantitative representation of the increase or decrease of the considered parameters.

In addition to the MK trend test, the linear regression method is widely used for trend analysis since it is parametric, and the need for a dataset of a normally-distributed time series to perform the test can be considered a weakness. However, among the various time-series trend detection tests, the MK test has become the most commonly-used trend test due to its simplicity, ability to handle non-normal and missing data distribution, and ability to control the effects of outliers and eliminate gross data errors. Furthermore, the trend test can be used for different time frames, such as monthly, seasonal, or annual.

The MK trend test has been done in a series, where n is the length of the sample, x_i and x_j are from $i = 1, 2, \ldots\ n-1$ and $j = i+1, \ldots\ n$. The MK statistics "S" can be calculated by the following Equations (1) and (2).

$$S = \sum_{i=1}^{n-1} \sum_{j=i+1}^{n} sgn(x_j - x_i) \tag{1}$$

$$sgn\ (x_j - x_i)\ = \left\{ \begin{array}{c} +1, > (x_j - x_i), \\ 0, = (x_j - x_i), \\ -1, < (x_j - x_i) \end{array} \right\} \tag{2}$$

If the number of records used for the test is greater than 10 (N > 10), then the average distribution statistic is approximately equal to zero, and the variance of "S" is calculated using Equation (3). Usually, more than 10 records are used to analyze the trend of the time series.

$$Var(s) = \frac{n(n-1)(2n+5) - \sum_{i=1}^{m} t_i(i)(i-1)(2i+5)}{18} \tag{3}$$

where t_i is the number of records specified in sample i, then, MK's statistics Zc (standard average deviation) for N > 10 can be calculated with values of "S" and $Var(S)$ using Equation (4).

$$Zc = \left\{ \begin{array}{c} \frac{S-1}{\sqrt{Var(S)}}, \quad S > 0, \\ 0, \quad S = 0, \\ \frac{S+1}{\sqrt{Var(S)}}, \ S < 0. \end{array} \right\} \tag{4}$$

Zc is used to assess whether there is a statistically significant trend or not. A positive Zc value depicts an increasing trend, while the negative Zc data gives a decreasing trend for the period. Since the test is two-tailed, $|Zc| > z\alpha/2$, the null hypothesis is rejected, while α is the significance level for the test. Positive values of Zc show an increasing trend, and negative values denote a decreasing trend for the particular parameter.

In this study, the two-tailed MK trend test was used to identify annual and monthly rainfall trends for countries, river basins, climatic zones, and provinces in the African Continent with a 5% significance and 95% confidence level.

2.3.3. Sen's Slope Estimate

Since the MK test shows either positive or negative increases, Sen's slope estimate can be used as a statistical test together with the MK test to determine the magnitude of that decrease or increase the trend. Sen's slope shows the increase and decrease of the slope magnitude corresponding to the MK values. If a linear trend in the dataset is considered, the true slope is estimated using a simple non-parametric and systematic procedure [73].

Slope pairs can be calculated for all data using the following Equation (5):

$$Ti = \frac{x_j - x_k}{j - k}\ for\ i = 1, 2, 3, \ldots\ldots n,\ j > k, \tag{5}$$

where, *Ti* is the slope and x_j, and x_k are the data values at time j and k, respectively. The mean of the n values of *Ti* is encoded as Sen's slope estimator (*Qi*) and is calculated using Equation (6).

$$Qi = \begin{cases} \left(T_{(n+1/2)}\right), & n \text{ is odd}, \\ \frac{1}{2}\left(T_{(n/2)} + T_{(n+2)/2}\right), & n \text{ is even} \end{cases} \quad (6)$$

3. Results

The section focuses on detailed statistical presentations of annual rainfall for different geographical units, in the form of climate zones, major river basins, regions, and countries, and analyzes spatial and temporal changes in long-term monthly, seasonal, and annual rainfall at the continental scale.

3.1. Long-Term Monthly Rainfall Distribution in Africa

Although Africa has two monsoon seasons, WAM and EAM, the spatial propagation of monthly rainfall varies gradually across months (Figure 2). From June to September (i.e., WAM) the heavy rainfall occurs above the equator from west to east and this period usually receives the highest rainfall, which is more than 250 mm per month. On the other hand, Figure 2 depicts that EAM activation causes increases in rainfall south of the equator from March to May and from November to December.

However, countries above northern latitudes (15°N) receive less than 35 mm of rainfall each month throughout the year, with zero rainfall in most months, and countries below the equator do not receive more than 35 mm of rainfall during six months (i.e., May to September). Furthermore, countries around southern latitudes (15°S) experience severe dry weather from June to August, especially in Madagascar, which experiences up to seven months of dry weather. The most striking finding of a change in monthly rainfall is that Madagascar and the coastal countries of Northeast Africa receive significantly higher rainfall from December to March.

3.2. Long-Term Seasonal Rainfall Distribution

In order to study seasonal rainfall behavior, as depicted in Figure 3, daily TAMSAT data were accumulated into the timeframe of December–February (DJF), March–May (MAM), June–August (JJA), and September–November (SON). As represented in the long-term spatial distribution of seasonal rainfall in Figure 3b,d, the western and eastern regions receive more than 1000 mm of rainfall in some parts in JJA and DJF, while the northern and southern regions receive less than 130 mm of rainfall in all four seasons. Madagascar receives high rainfall during the DJF season, while only countries between 0–15°N latitudes from the equator receive high rainfall during the JJA season (Figure 3b). The other noteworthy finding is that almost all the countries in Central Africa, except Chad, receive more than 350 mm of rain in all four seasons, while the countries around 15°S latitude receive zero rainfall in JJA (Figure 3b). Despite the spatial distribution of monthly and seasonal rainfall, a detailed study of their trends is more appropriate to gain a clearer understanding of their long-term rainfall variability. Therefore, in this study, the annual rainfall variability and trends were also discussed as indicating climate change.

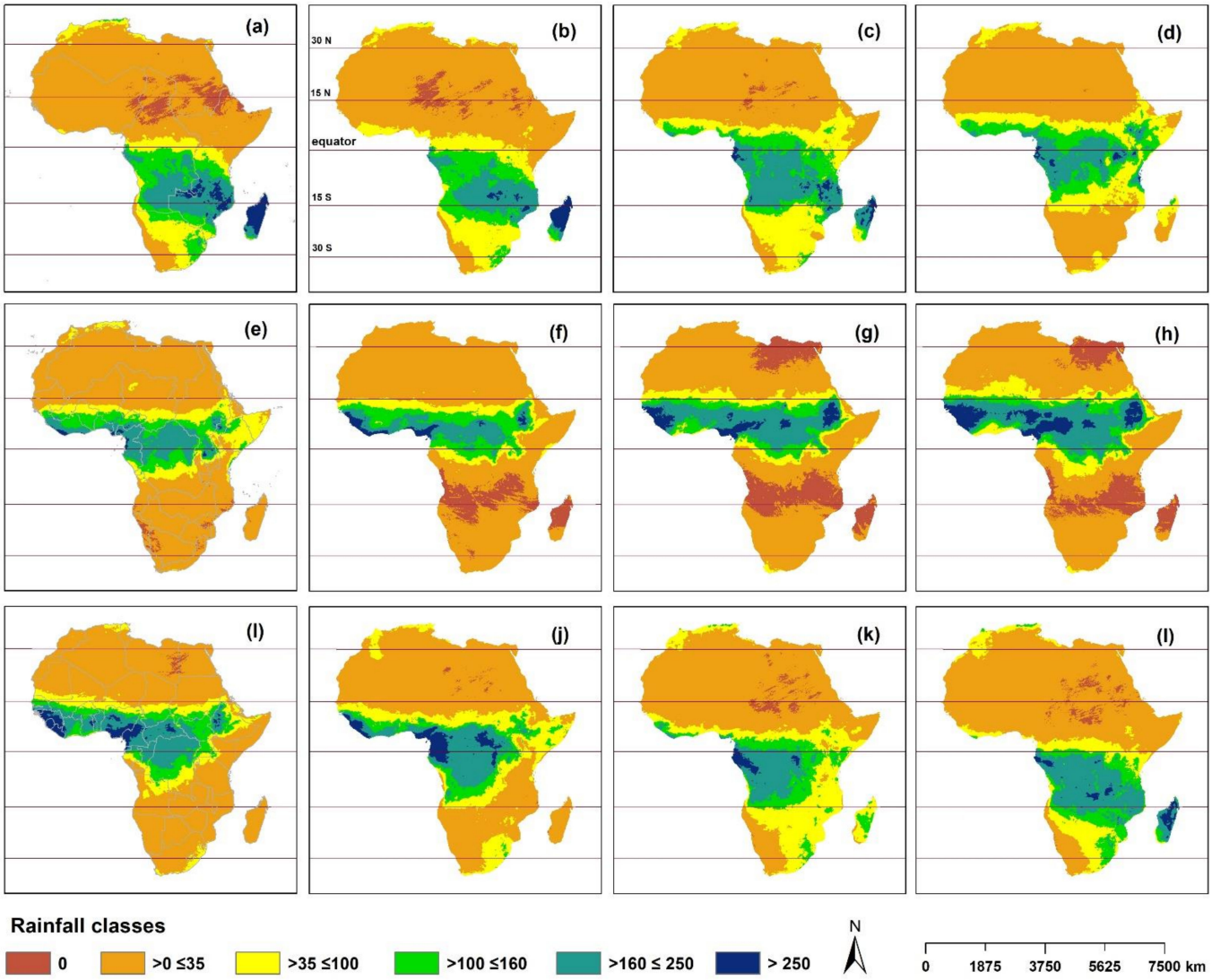

Figure 2. Spatial distribution of monthly average rainfall (mm) across Africa from 1983 to 2020. (**a**) January, (**b**) February, (**c**) March, (**d**) April, (**e**) May, (**f**) June, (**g**) July (**h**) August, (**i**) September, (**j**) October, (**k**) November and (**l**) December.

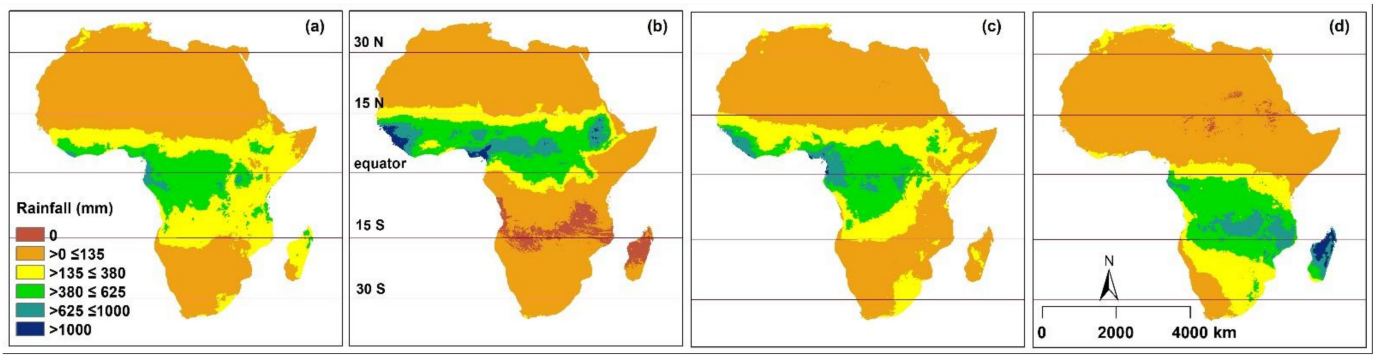

Figure 3. Spatial distribution of seasonal average rainfall (mm) across Africa from 1983 to 2020. (**a**) March–April–May (MAM), (**b**) June–July–August (JJA), (**c**) September–October–November (SON) and (**d**) December–January–February (DJF).

3.3. Long-Term Annual Rainfall Distribution

Long-term seasonal rainfall studies have shown that regions closest to the equator receive higher rainfall in both the September–November and March–May timeframes. The main reason for this is that ITCZ covers areas close to the equator twice a year (Bimodal rainfall). The spatial distribution of long-term average annual rainfall is close to that of monsoon rainfall. As represented in Figure 4, Africa's highest average annual rainfall is over 2000 mm, which is received near the equator. As the ITCZ shifts away from the equator, a sharp decrease in annual rainfall is observed, and the main reason is being that those areas receive rainfall only in one monsoon season (unimodal rainfall). Even though more than 80% of the area in Northern Africa receives less than 250 mm of average annual rainfall, Southern Africa received relatively higher rainfall compared to Northern Africa.

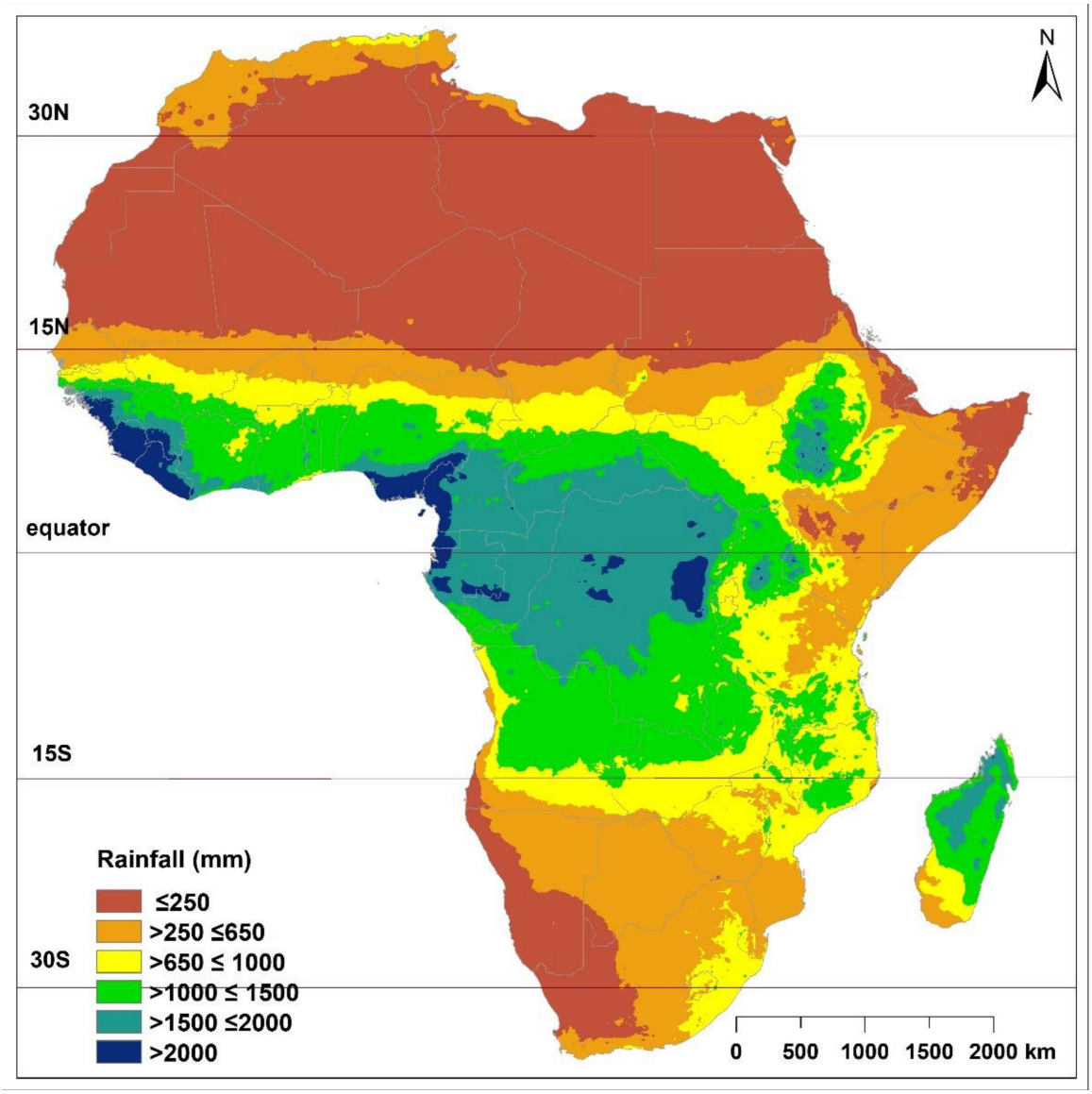

Figure 4. Spatial distribution of annual average rainfall (mm) across Africa from 1983 to 2020.

3.4. Country-Level Annual Rainfall Variability from 1983 to 2020

Annual rainfall varies across countries because of climatic variability over time. In order to understand these changes, it is appropriate to represent the spatial distribution of rainfall over time. Figure 5 shows the spatial distribution of all countries in Africa using the country's average rainfall values calculated for each year from 1983 to 2020. Theoretically,

rainfall can be divided into any number of classes, but Figure 4 shows six classes that are generated using the percentile classification approach to detect temporal variation in annual rainfall at the country level. The percentile classification approach was used to classify country-level rainfall data, taking into account 2090 data records calculated to cover 54 countries from 1983 to 2020 into categories of 10%, 30%, 50%, 70%, 90%, and 90–100%.

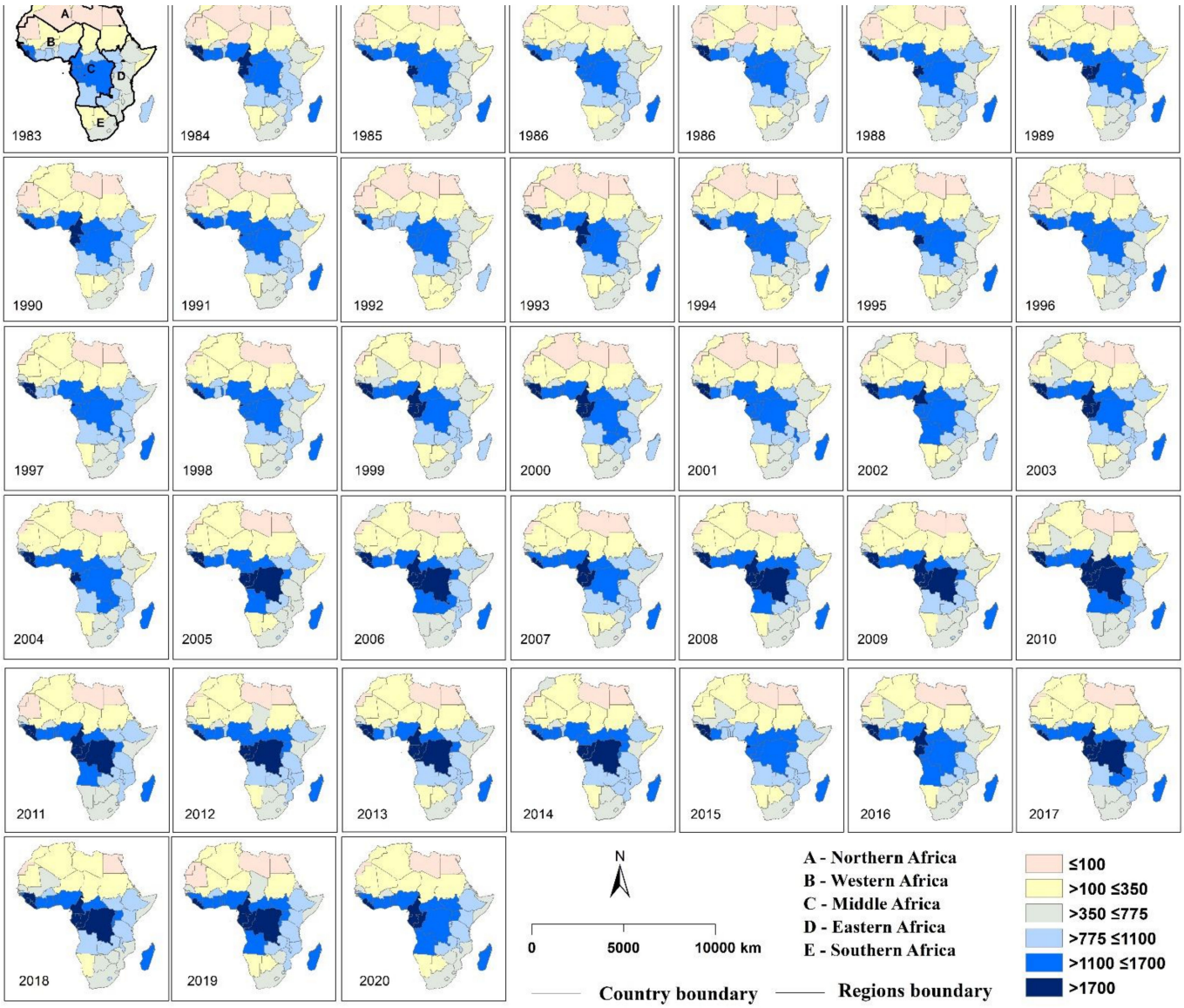

Figure 5. Changes in African countries' annual average rainfall from 1983 to 2020.

However, the remarkable thing that the above classification methodology can identify is that after the year 2000 it has been confirmed that the annual rainfall in most countries of Central Africa exceeds the 1700 mm rainfall limit. Moreover, the countries of Algeria, Tunisia, Mali, Niger, and Western Sahara in the North and East African regions show a clear increase in annual average rainfall. Overall, the peculiarity shown is that countries in the Southern African region and most other countries except Egypt, Libya, and Madagascar show an increase in annual average rainfall. It is essential to analyze further whether this increase is significant or not, as it will be of great help in determining climate resilience in Africa.

3.5. Time-Series Rainfall Variability Comparison of Countries with Reference to African Regions

Figure 6 shows the variation in annual average rainfall from 1983 to 2020 in the northern, western, central, and southern regions of Africa together with the countries which belong to the same region. Furthermore, rainfall variability usually shows different patterns, but overall expresses a tendency to increase in rainfall. About 70% (n = 11) of the countries in the western region (Figure 6a) have an average annual rainfall higher than the average in that region. However, the number of countries belonging to the northern (Figure 6d) and southern regions (Figure 6c) is relatively low, and approximately 50% (n = 5) of the countries can be identified as both above and below the annual average rainfall in their region.

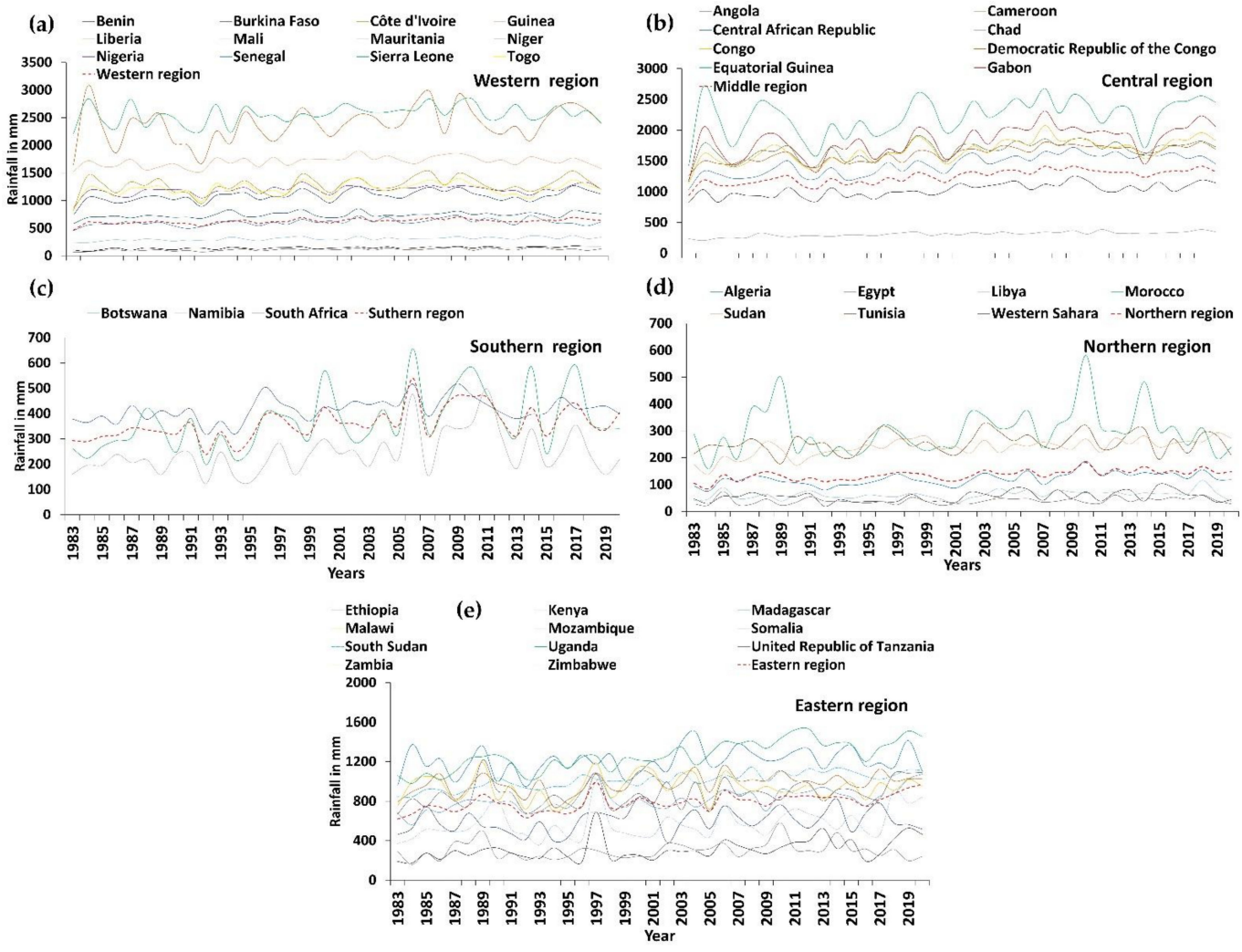

Figure 6. Time-series rainfall representation of African countries belonging to a particular region in between 1983 and 2020. (**a**) Western region, (**b**) Central region, (**c**) Southern region, (**d**) Northern region and (**e**) Eastern region.

In the Central Africa region (Figure 6b), only Chad and Angola have lower than average annual rainfall in the region, especially in Chad, which has as low as 700–1000 mm compared to other countries of the region. Rainfall in the African countries of the Eastern region (Figure 6e) shows a mixed behavior of the rainfall variability, with rainfall patterns in different countries tending to coincide with each other compared to other regions. However, between 40% and 60% (n = 6 and n = 8) of the countries of East Africa have fallen on both sides of the region's average rainfall.

3.6. Descriptive Statistics

A detailed analysis of rainfall variability across all geographical regions, including country, major river basins, climate zone and regions of Africa (Tables 1, 2, A1 and A2) indicates that tropical rainforests in central Africa receive maximum annual rainfall (more than 2000 mm), while the northern part of the Northern African region receives the minimum rainfall (less than 140 mm). However, some countries, river basins, and climate zones in Western, Eastern, and Southern Africa are experiencing declining rainfall. Out of the total 48 countries studied, 22 countries receive less than 750 mm of rainfall (desert to arid), and only 11 countries receive more than 1250 mm of rainfall (Tropical), while 15 countries receive between 750 and 1250 mm of rainfall (semi-arid to semi-humid). The highest recorded annual average rainfall in an African country in the last 37 years was 3075.2 mm in Liberia (in 1984), and the lowest in Western Sahara was 18.7 mm (in 1992).

Table 1. Descriptive statistics for annual rainfall (in mm) for Africa's climate zones from TAMSAT data (1983 to 2020).

Climate Zone	Average	Max	Min	STD	CV	Median
Tropical Grass Land	1120.4	1294.3	861.0	88.3	7.9	1141.9
Sub-tropical North Desert	246.2	400.9	178.4	46.4	18.8	240.5
Tropical Northern Desert	74.1	108.6	38.2	14.9	20.1	71.8
Tropical Northern Semi-arid	445.1	542.9	293.9	51.5	11.6	445.3
Tropical Rainforest	1793.0	2108.6	1325.0	165.7	9.2	1820.0
Southern Tropical Semi-arid	810.5	971.4	611.0	84.1	10.4	817.0
Southern Tropical Desert	271.3	514.1	138.9	87.6	32.3	249.1
Sothern Sub-Tropical Desert	400.7	521.3	289.5	52.3	13.1	396.0
Sothern Sub-Tropical Humid	549.9	641.6	445.2	48.9	8.9	550.4
Tropical Grass Land (MA *)	1146.1	1418.0	886.0	135.2	11.8	1140.1
Tropical Northern Semi-arid (MA *)	523.9	771.0	268.0	116.3	22.2	529.0
Northern Sub-tropical Humid	447.9	662.6	317.0	82.9	18.5	441.4
Tropical Rainforest (MA *)	1411.1	1779.9	910.6	179.2	12.7	1402.8

* Madagascar (MA).

The most striking feature of the detailed statistical analysis is that almost all countries, river basins, and climatic zones in the Northern and Southern African regions, which receive significantly less rainfall, have a higher (>15) Coefficient of Variance (CV). This indicates that there is a high probability of occurrence of extreme rainfall (either low or high) in those regions. Furthermore, the analysis shows that only eight countries had CV values of less than 10, with 18 counties having CV values of more than 15, but the highest number of countries with 22 had CV values between 10 and 15 (Table A1). The extraordinary representation is that the CV value of the Namibian coastal basin is about 159.7, which is the largest among all the geographies. One other important point to note in the study of Africa's rainfall variability is that the majority of the area in Central Africa receives rainfall above 2000 mm, and the CV value is less than 10, indicating that they exhibit stable tropical climates in accordance with the Köppen climate classification [74].

According to the standard classification of CV, rainfall received for nine river basins out of 25 have high variability, which indicates a higher probability for extreme weather events. However, Niger, Nile, and Senegal river basins receive 666.93 mm, 651.98 mm, and 492.57 mm average rainfalls, respectively, with low CV values, indicating steady rainfall patterns. In particular, the study of spatial and temporal variability in rainfall can provide an overall perspective of the rainfall variability over the entire African continent.

Table 2. Descriptive statistics for Africa's annual rainfall (in mm) for major river basins from TAMSAT data (1983 to 2020).

River Basins	Average	Max	Min	STD	CV	Median
Africa, East Central Coast	817.3	1110.9	580.3	126.7	15.5	778.2
Africa, Indian Ocean Coast	649.0	1036.3	373.3	157.6	42.2	666.9
Africa, North Interior	73.4	112.3	41.1	15.3	37.2	73.6
Africa, North West Coast	166.8	293.7	86.4	41.4	47.9	162.4
Africa, Red Sea-Aden Coast	201.9	375.6	102.7	56.0	54.5	187.4
Africa, South Interior	499.4	804.9	285.6	118.4	41.5	468.9
Africa, West Coast	1527.6	1787.6	1120.9	140.0	12.5	1532.7
Angola, Coast	912.6	1151.1	717.9	113.8	15.8	942.4
Congo	1538.5	1740.0	1184.1	130.4	8.5	1573.7
Gulf of Guinea	1871.1	2233.2	1234.1	219.4	17.8	1892.0
Lake Chad	356.0	431.6	259.5	41.9	11.8	364.4
Limpopo	451.2	656.3	266.0	101.4	38.1	456.2
Madagascar	1211.6	1501.9	945.5	132.6	14.0	1203.3
Mediterranean South Coast	292.6	399.7	218.1	47.4	21.7	284.0
Namibia, Coast	116.5	346.1	40.8	65.2	159.7	110.4
Niger	666.9	755.8	519.3	44.7	6.7	671.5
Nile	652.0	763.1	486.3	61.1	9.4	659.0
Orange	304.9	452.2	196.7	55.9	18.3	300.4
Rift Valley	734.1	983.4	532.6	99.4	18.7	714.0
Senegal	492.6	578.8	404.2	42.9	8.7	489.6
Shebelli–Juba	488.4	1015.6	308.7	150.6	48.8	454.7
South Africa, South Coast	560.2	656.6	451.2	46.8	10.4	561.5
South Africa, West Coast	183.1	290.9	113.5	48.9	43.1	169.4
Volta	959.3	1101.7	689.7	74.5	10.8	961.2
Zambezi	884.2	1050.1	643.6	100.0	11.3	895.7

4. Discussion

This section focuses mainly on interpreting rainfall variability and trends for the different timeframes (monthly, seasonal and annual) and geographical units (regions, climate zones, river basins, and countries) used in the study.

4.1. Annual and Monthly Rainfall Trend of African Regions

The annual rainfall variability generated by the MK trend test for the northern, eastern, central, southern, and western regions is shown in Figure 7. The MK trend test results show that there is a significant increase in rainfall in all the African regions. Subsequently, Sen's slope analysis confirms that the maximum annual rainfall increase is 6.84 mm/year in the Central Region, and the lowest increase of 1.07 mm/year is in the Northern region. Although the relative magnitude of the annual increase in rainfall in the Northern region is small (1.07 mm/year), the most favorable condition is the statistically significant increase in rainfall. The other important finding is that the annual rainfall trend at the regional level is increasing as high as 4.62 mm/year in the Eastern region.

Even though a clear increase in annual rainfall can be identified as earlier described, a detailed investigation of future changes in long-term monthly rainfall trends can provide the information needed to properly implement approaches to food security, such as agricultural crop and water management. Figure 8 shows the spatial distribution of Kendall's Tau (uniform tendency in a linear increase or decrease) and Sen's slope values (positive and negative values indicate increasing and decreasing trends, respectively) of the monthly rainfall in Africa at the regional level. The important point in the monthly rainfall trends analysis is that in most months, except January, July, September, and October, there is an increase in rainfall in every region at different scales. The northern, eastern, and southern regions also showed a decrease in rainfall during January, July, September, and October, respectively, but it did not show a statistically significant decrease in rainfall as per the MK trend test results.

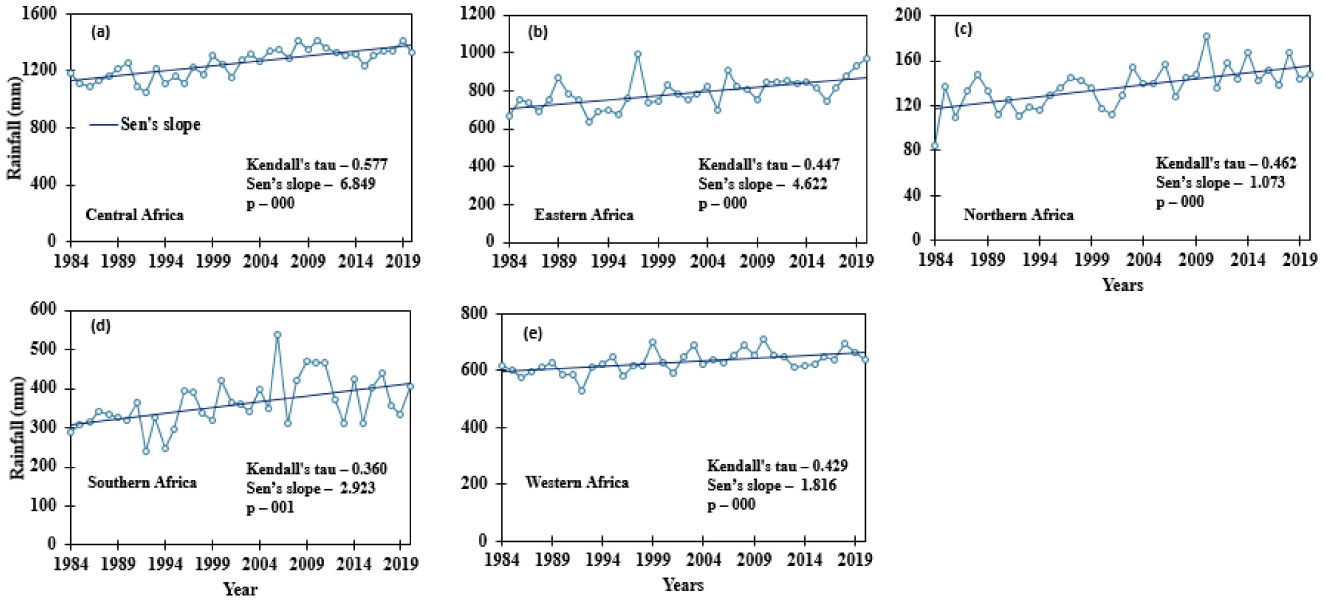

Figure 7. Annual rainfall trend for regions in Africa (**a**) Central region, (**b**) Eastern region, (**c**) Northern region, (**d**) Southern region and (**e**) Western region.

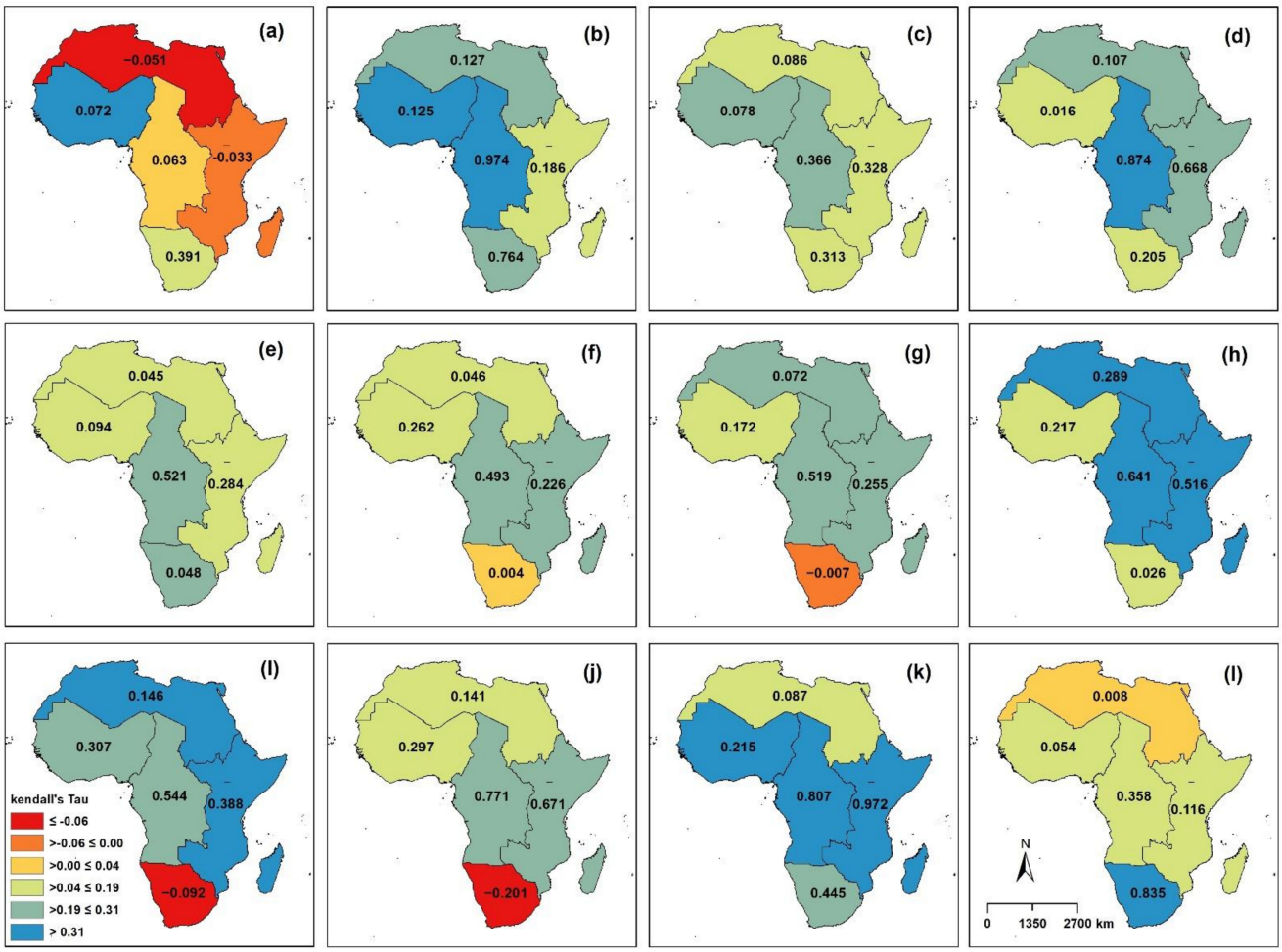

Figure 8. Kendall's Tau (colour gradient) and Sen's slope (numbers) for monthly rainfall trends for five African regions between 1983 and 2020. (**a**) January, (**b**) February, (**c**) March, (**d**) April, (**e**) May, (**f**) June, (**g**) July, (**h**) August, (**i**) September, (**j**) October, (**k**) November and (**l**) December.

The farmers should pay careful attention to their agricultural activities during the West African Monsoon (WAM) as there is a high potential of increasing the drought vulnerability due to declining rainfall in the southern region during the WAM season. However, during the East African monsoon, especially during the long (March–May) and short (October–December) rainy seasons, almost all the regions (except the southern region in October) show an increasing trend in rainfall. The other major finding of this monthly data analysis is that the increase in rainfall in any given month does not exceed 1 mm/month, indicative of high drought vulnerability.

4.2. Annual and Monthly Rainfall Trend of Climatic Zones

In Africa, 13 climate zones can be identified as Tropical Grass Land, Sub-tropical North Desert, Tropical Northern Desert, Tropical Northern Semi-arid, Tropical Rainforest, Southern Tropical Semi-arid, Southern Tropical Desert, Southern Sub-Tropical Desert, Southern Sub-Tropical Humid, Tropical Grass Land Madagascar, Tropical Northern Semi-arid Madagascar, Northern Sub-tropical Humid and Tropical Rainforest Madagascar. Through this study, the rainfall behavior of the climate zone of the African mainland and Madagascar was studied separately. Figure 9 shows Kendall's Tau, Sen slope, and *p*-value of the annual rainfall trend analysis for each climate zone, except Tropical Rainforest Madagascar. As per Figure 9, except for the climate zones of Sub-tropical North Desert (b), Southern Sub-Tropical Humid (i), Northern Sub-tropical Humid (l), and Madagascar (i, k), there is a statistically significant rainfall trend in all the other zones. The Tropical Rainforest (Figure 9e zone shows the maximum annual increase in rainfall of 8.21 mm/year and followed by an increase of 5.32 mm/year, 3.17 mm/year, 2.85 mm/year, and 2.50 mm/year in the Tropical Grass Land (a), Tropical Northern Semi-arid (d), Southern Tropical Desert (g), and Southern Tropical Semi-arid zones (f), respectively. This implies that these climate zones have become wetter, and in some cases, experience extreme weather events of floods, which destroy infrastructure and animal habitats and result in loss of human and animal life, while in other cases the increases in rainfall suggest that they have potentially become more productive.

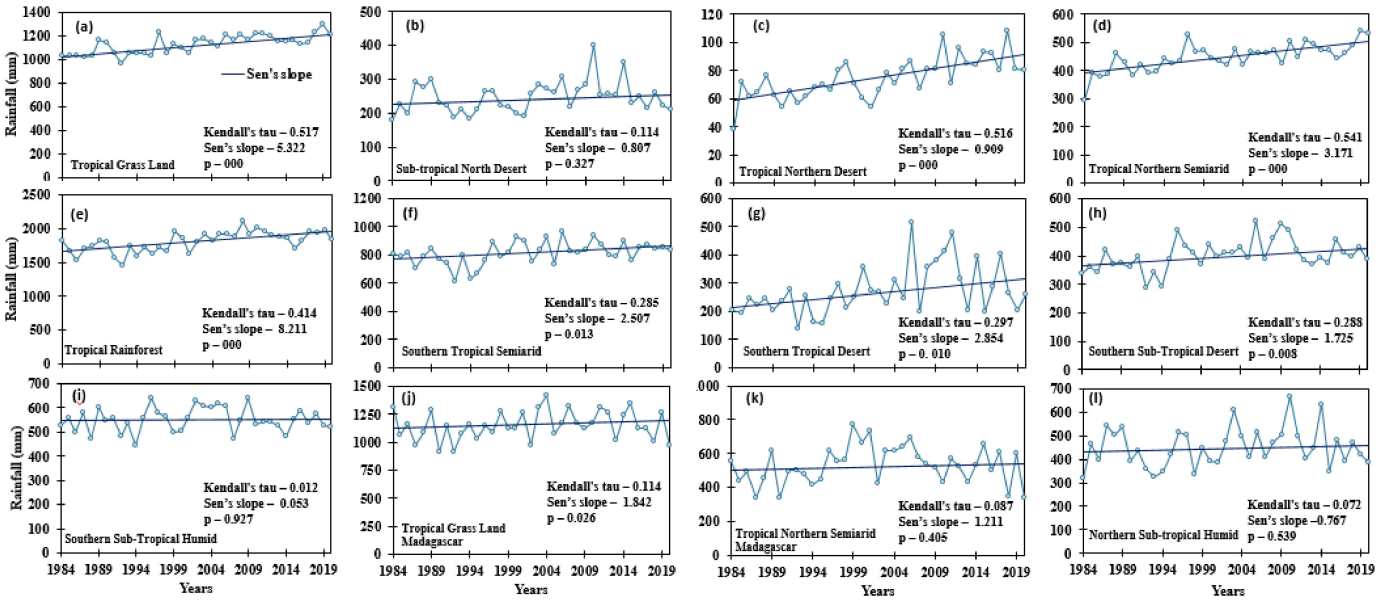

Figure 9. Annual rainfall trend for different climate zones (**a**) Tropical Grass Land, (**b**) Sub-tropical North Desert, (**c**) Tropical Northern Desert, (**d**) Tropical Northern Semi-arid, (**e**) Tropical Rainforest, (**f**) Southern Tropical Semi-arid, (**g**) Southern Tropical Desert, (**h**) Southern Sub-Tropical Desert, (**i**) Southern Sun-Tropical Humid, (**j**) Tropical Grass Land—Madagascar, (**k**) Tropical Northern Semi-arid—Madagascar and, (**l**) Northern Sub-Tropical Humid in Africa, including Madagascar.

Different trends can be identified when analyzing the monthly rainfall variability in the climatic zones, as shown in Figure 10. The implication is that during the West African Monsoon (WAM), from June to October, the climate zones south of 15° S latitudes (i.e., Southern Tropical Semi-arid, Southern Tropical Desert, Southern Sub-Tropical Desert, and Sub-Tropical Humid) show a tendency to decrease rainfall (Kendall's tau ≤ -0.06). However, especially during the East African Monsoon (EAM), it can be pointed out that almost all climate zones have an increasing trend in rainfall. In both WAM and EAM, most climate zones above 15°S latitude each month shows an increasing trend in rainfall with a statistical significance. However, the monthly rainfall trend is less than 1 mm/month.

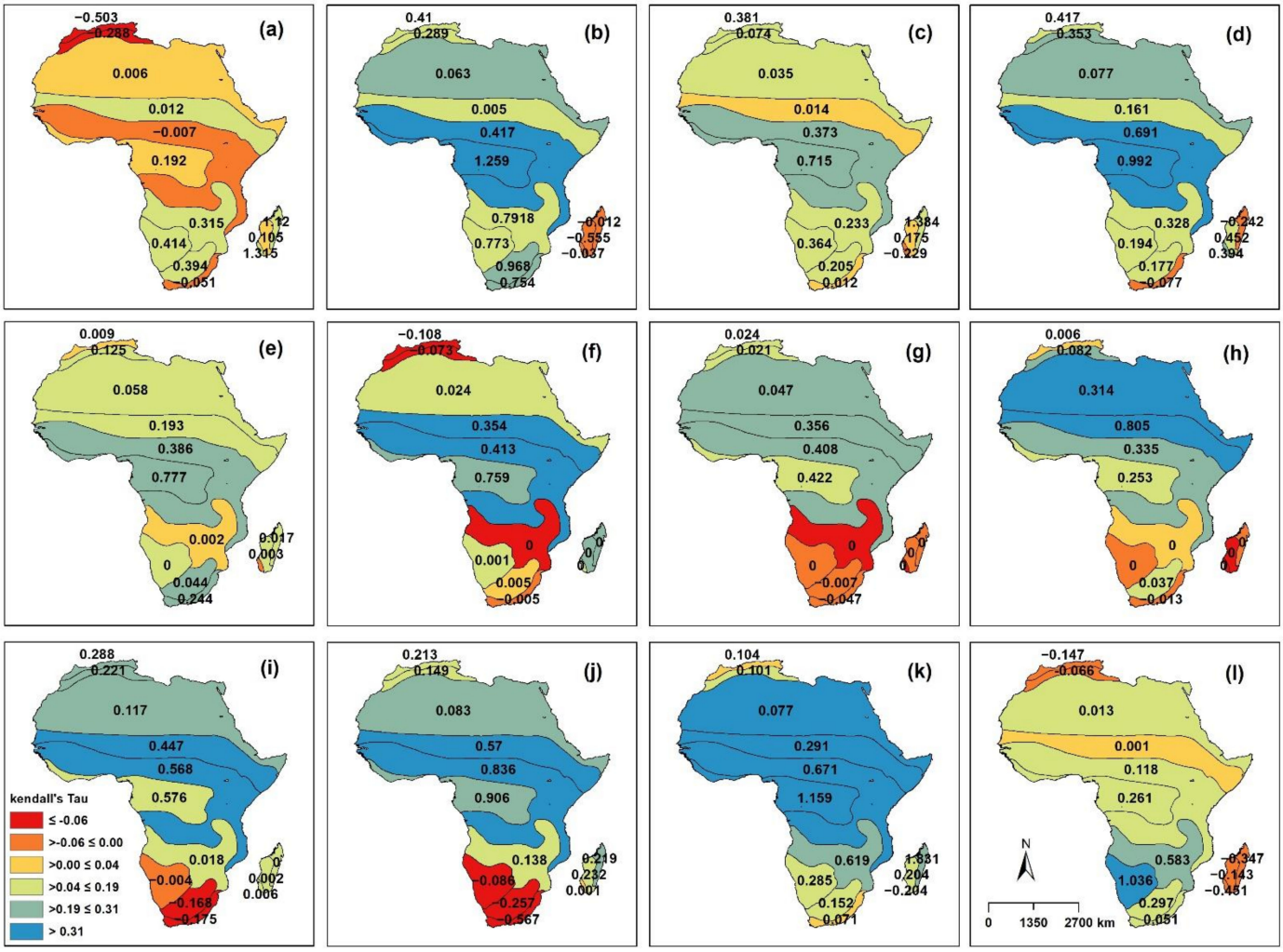

Figure 10. Kendall's Tau (colour gradient) and Sen's slope (numbers) for monthly rainfall trends in different climate zones of Africa including Madagascar between 1983 and 2020. (**a**) January, (**b**) February, (**c**) March, (**d**) April, (**e**) May, (**f**) June, (**g**) July (**h**) August, (**i**) September, (**j**) October, (**k**) November and (**l**) December.

4.3. Annual Rainfall Trend in Major River Basins and Countries

The previous sections analyzed and interpreted the annual, monthly, and seasonal rainfall trends for all the geographical units, including river basins and countries. Since the seasonal rainfall increases were shown for the Gulf monthly intervals represent rainfall trends for short and medium timeframes, the analysis of annual rainfall variability provides trends for the long timeframe, critical for long-term planning. Figure 11 provides more insights into the spatial distribution of annual rainfall trends at the river basin and country

level, while Tables 3 and 4 show Kendal's Tau values, Sen's slopes, and *p*-values of each river basin and country.

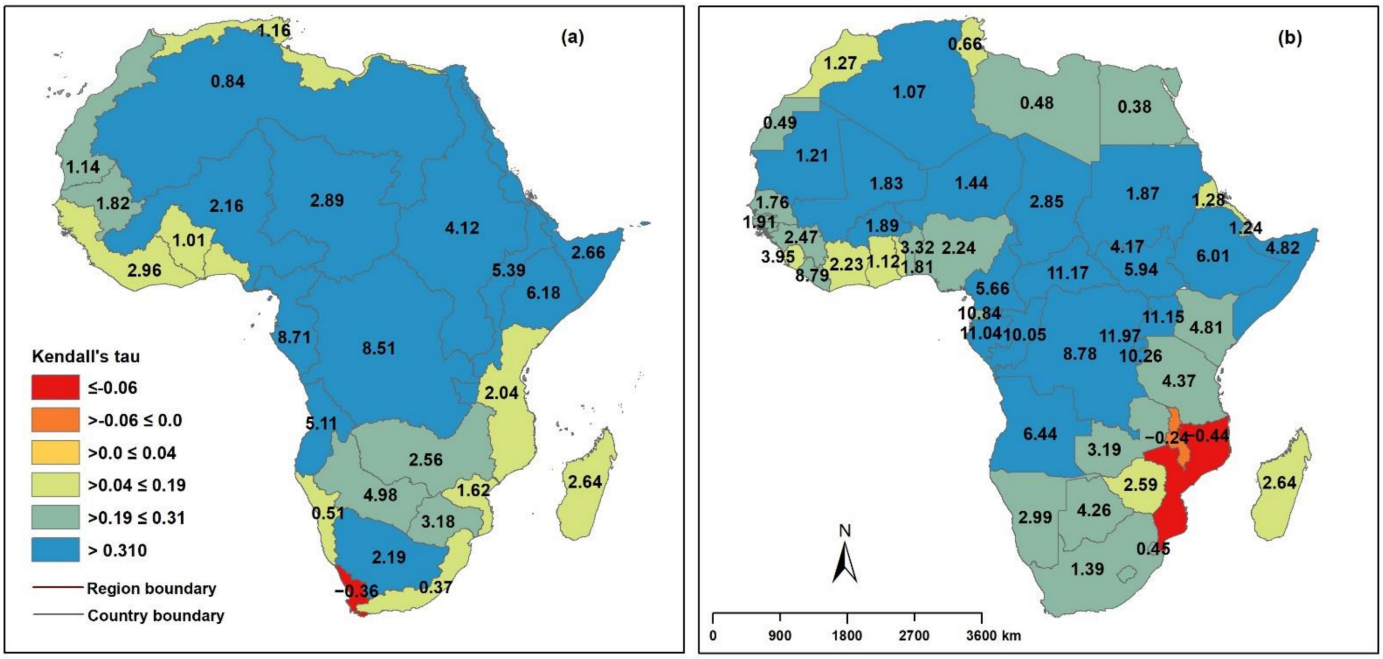

Figure 11. Annual rainfall trend with Kendall's Tau (colour gradient) and Sen's slope (numbers) between 1983 and 2020. (**a**) major river basins, and (**b**) countries of Africa.

Except for the West Coast river basin of Africa, all the other river basins show an increasing rainfall trend with about 50% of those river basins showing a statistically significant increase (Table 3). The two river basins called the Gulf of Guinea and the Congo show the highest annual rainfall increases of 8.713 mm/year and 8.512 mm/year, respectively. Furthermore, the analysis suggests that the increased rainfall in the river basins in the Sothern and Eastern regions is less than in the river basins in the northern, western, and central regions. The study reveals that although the maximum annual rainfall increases were shown for the Gulf of Guinea and the Congo basins, the strongest annual rainfall increase trend emerged in the Nile and Lake Chad river basins in the northern tropical desert and tropical northern semi-arid climate zone. Interpreting the spatial distribution of rainfall trend of river basins, the overall increase in rainfall in coastal regions, except the western and northeastern coasts, is significantly less than inland river basins.

Table 3. Kendall's Tau, *p*-value, and Sen's slope for annual rainfall (1983–2020) for major African river basins. Bold numbers in *p*-values represent the statistically significant trend.

Basin Name	Kendall's Tau	*p*-Value	Sen's Slope
Africa, East Central Coast	0.147	0.205	2.036
Africa, Indian Ocean Coast	0.087	0.381	1.619
Africa, North Interior	0.441	**<0.001**	0.842
Africa, North West Coast	0.198	0.087	1.141
Africa, Red Sea—Gulf of Aden Coast	0.447	**<0.001**	2.658
Africa, South Interior	0.315	**0.006**	4.977
Africa, West Coast	0.168	0.147	2.962
Angola, Coast	0.330	**0.001**	5.112

Table 3. *Cont.*

Basin Name	Kendall's Tau	*p*-Value	Sen's Slope
Congo	0.565	**<0.001**	8.512
Gulf of Guinea	0.321	**0.005**	8.713
Lake Chad	0.679	**<0.001**	2.895
Limpopo	0.222	0.055	3.184
Madagascar	0.156	0.178	2.643
Mediterranean South Coast	0.171	0.139	1.158
Namibia, Coast	0.084	0.472	0.506
Niger	0.453	**<0.001**	2.161
Nile	0.610	**<0.001**	4.124
Orange	0.324	**0.005**	2.200
Rift Valley	0.426	**0.001**	5.394
Senegal	0.309	**0.007**	1.825
Shebelli—Juba	0.360	**0.002**	6.182
South Africa, South Coast	0.075	0.522	0.367
South Africa, West Coast	−0.081	0.507	−0.360
Volta	0.120	0.301	1.005
Zambezi	0.198	0.087	2.558

Analysis of rainfall trends from river basin to country level finds that the number of countries showing a statistically significant increase in trend is about 68% (Table 4). South Sudan and Chad show the highest rainfall trend of 0.61 and 0.62, respectively. However, the increase in annual rainfall of those two countries is shown to be more variable at 2.84 mm/year and 5.93 mm/year (Table 4), as the two countries are located in two different climate zones. Additionally, the Kendall's Tau (Zc) value of more than 0.41 in Angola, Burundi, Central African Republic, Chad, Congo, Ethiopia, Mali, Mauritania, Niger, Rwanda, South Sudan, Sudan, Uganda, and the Democratic Republic of the Congo indicates that those countries have the statistically significant increasing trends in rainfall.

Table 4. Kendall's Tau, *p*-value, and Sen's slope for annual rainfall for African countries (1983–2020). Bold numbers in *p*-values represent the statistically significant trend.

Country	Kendall's Tau	*p*-Value	Sen's Slope	Country	Kendall's Tau	*p*-Value	Sen's Slope
Mozambique	−0.027	0.794	−0.437	South Africa	0.261	**0.024**	1.389
Malawi	−0.021	0.842	−0.238	Kenya	0.264	**0.022**	4.800
Ghana	0.051	0.666	1.116	Nigeria	0.291	**0.012**	2.241
Togo	0.105	0.367	1.802	Benin	0.306	**0.008**	3.318
Tunisia	0.108	0.168	0.663	Botswana	0.315	**0.006**	4.261
Sierra Leone	0.117	0.314	3.950	Cameroon	0.336	**0.004**	5.656
Zimbabwe	0.126	0.278	2.592	Burkina Faso	0.342	**0.003**	1.900
Morocco	0.135	0.244	1.267	Gabon	0.348	**0.003**	11.041
Côte d'Ivoire	0.138	0.234	2.230	Algeria	0.366	**<0.001**	1.070
Madagascar	0.156	0.178	2.638	Somalia	0.387	**0.001**	4.816
Eritrea	0.177	0.126	1.278	Mauritania	0.435	**<0.000**	1.207
Western Sahara	0.186	0.108	0.493	Ethiopia	0.444	**<0.001**	6.003
Guinea	0.201	0.082	2.468	Mali	0.468	**<0.001**	1.826
Liberia	0.207	0.073	8.787	Angola	0.477	**<0.001**	6.442
Gambia	0.213	**0.045**	1.908	Congo	0.477	**<0.001**	10.046
Egypt	0.216	0.061	0.378	Rwanda	0.480	**<0.001**	11.973
Zambia	0.237	**0.040**	3.197	Burundi	0.483	**<0.001**	10.262

Table 4. *Cont.*

Country	Kendall's Tau	*p*-Value	Sen's Slope	Country	Kendall's Tau	*p*-Value	Sen's Slope
Zambia	0.237	**0.040**	2.923	Sudan	0.483	**<0.001**	1.872
Equatorial Guinea	0.240	**0.038**	10.842	Niger	0.526	**<0.001**	1.444
Libya	0.240	**0.038**	0.479	CAR **	0.550	**<0.001**	11.167
Namibia	0.246	**0.033**	2.988	DRC ***	0.565	**<0.001**	8.777
URT *	0.249	**0.031**	4.369	Uganda	0.598	**<0.001**	11.152
Senegal	0.252	**0.029**	1.757	Chad	0.607	**<0.001**	2.847
South Sudan	0.619	**<0.001**	5.937				

* United Republic of Tanzania (URT), ** Central African Republic (CAR), *** Democratic Republic of the Congo (DRC).

The magnitude of annual rainfall trends in Equatorial Guinea, Gabon, Congo, Rwanda, Burundi, Central African Republic, and Uganda increased by more than 10 mm/year, and those are countries particularly prone to receiving rain from both West African Monsoon and East African monsoon. All of these countries belong to the climate zones of tropical rainforests and tropical grasslands. Notably, the coastal countries of the Western African region generally received high rainfall with high intensity, but the rainfall trends in those countries did not increase significantly.

4.4. Seasonal Rainfall Trends by Regions, Climatic Zones, River Basins, and Countries of Africa

Although the annual and monthly rainfall trends show long-term and short-term patterns, seasonal trend analysis is more suitable for monitoring medium or inter-annual trends. Thus, the analysis of rainfall trends during four seasons March–May (MAM), June–August (JJA), September–November (SON), and December–January (DJF) for the four geographical units of regions, climate zones, major river basins, and countries in this study are shown in Figure 12. The most important indication is that during the JJA and SON seasons, areas below 15° S latitude show a decrease in rainfall compared to all other regions. Despite this declining trend, it is essential to note that this declining trend is not statistically significant.

Furthermore, the studies conducted by [75–77] have shown that some countries in East Africa have experienced a decrease in rainfall during the JJA period, and this study further confirms that there is a negative rainfall trend in countries adjacent to South Africa, such as Zimbabwe, Zambia, Malawi, and Mozambique. Even in the DJF, a declining rainfall trend can be detected in Malawi, Mozambique, and Madagascar, while there is a significant decrease in rainfall in the southern part of Eastern Africa during the MAM period. According to this seasonal rainfall occurrence, there is a significant increase in the rainfall in all seasons, especially in the northern areas of the Western and Northern African regions, and this finding has been confirmed by a study conducted through rainfall gauge data [78]. The most important point to highlight in the seasonal rainfall trends analysis of all these geographical units is the significant increase in rainfall over all countries, river basins, and climate zones in Central Africa, rendering them wetter over the years.

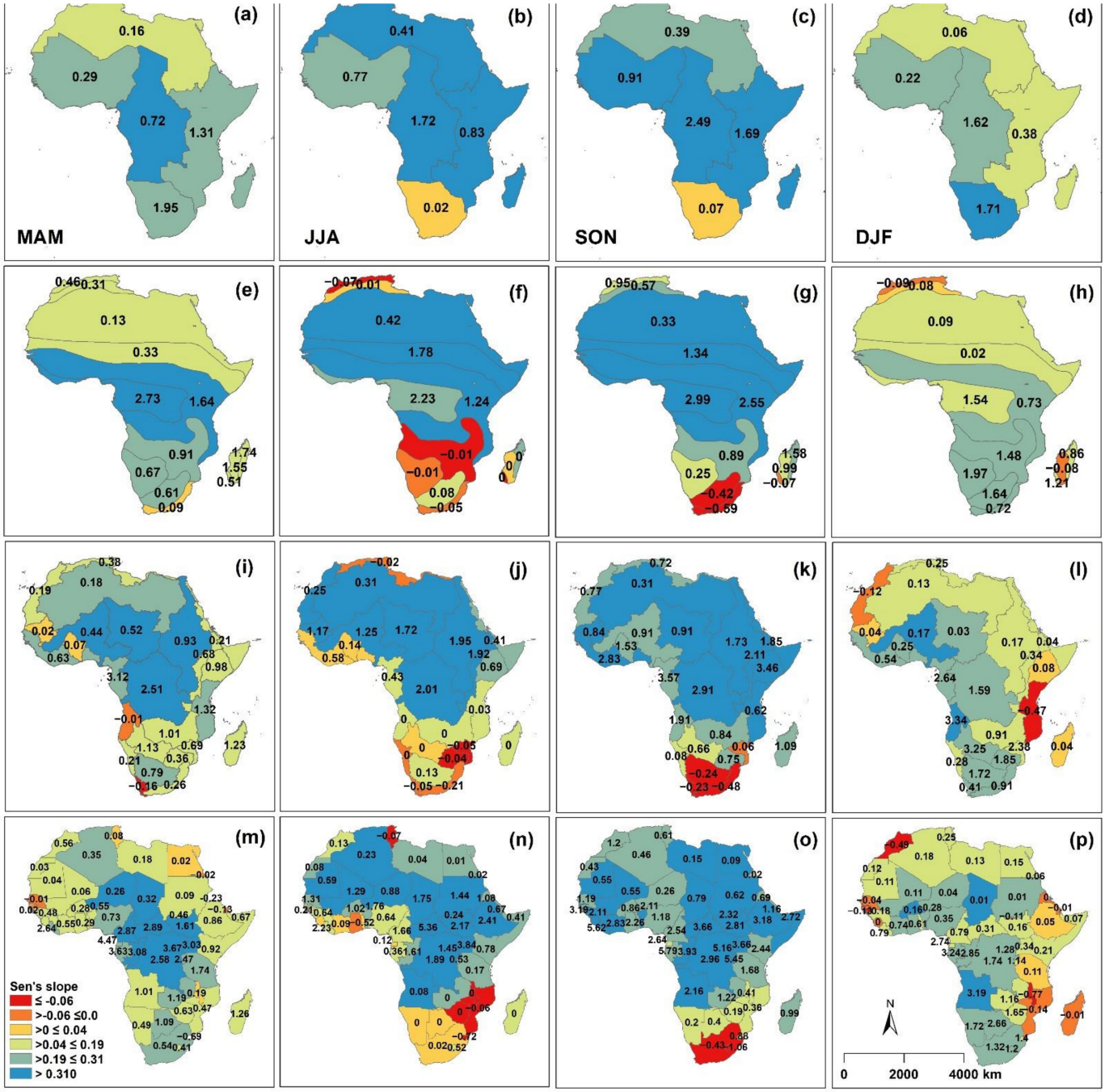

Figure 12. Kendall's Tau (colour gradient) and Sen's slope (numbers) as seasonal rainfall (MAM-March-May, JJA—June–August, SON—September–November, DJF—December–February) trends in between 1983 and 2020. (**a**) Regions in MAM, (**b**) regions in JJA, (**c**) regions in SON, (**d**) regions in DJF, (**e**) River basins in MAM, (**f**) River basins in JJA, (**g**) River basins in SON, (**h**) River basins in DJF, (**i**) Climate zones in MAM, (**j**) Climate zones in JJA, (**k**) Climate zones in SON, (**l**) Climate zones in DJF, (**m**) Countries in MAM, (**n**) Countries in JJA, (**o**) Countries in SON, (**p**) Countries in DJF.

5. Conclusions

Rainfall variability and trends across major climatic zones, regions, major river basins and countries in African Continent have been studied using TAMSAT data with a spatial resolution of 4 km. Very few studies on rainfall variability and trends in Africa have been conducted and they have primarily focused on the regional or local geographical context. Moreover, almost no studies cover the long-term variability and trend of rainfall over a

wide range of periods (monthly, seasonal, and annual) and in different geographical units (regions, climate zones, major river basins, and countries).

The analysis of the variability of monthly rainfall at the pixel level from 1983 to 2020 shows explicitly that any countries above 15°N and Below 15°S latitudes do not receive significant rainfall in any month. Countries located above 15°N latitudes do not receive more than 35 mm of rainfall in any month of the year. Country-level annual rainfall variability indicates that after 2000, the annual rainfall in most of the countries in the Central African region exceeded 1700 mm. However, Algeria, Tunisia, Mali, Niger, and Western Sahara in the Northern and Eastern African regions show an apparent increase in annual average rainfall from 1983 to 2020. The main conclusions drawn from the study of rainfall variability are that there is a significant increase in rainfall in the northern countries, but no significant change in the countries of the southern and eastern regions. In the countries and regions where this increase in annual rainfall occurs, agricultural crop diversification and systematic water management will have the potential to increase food production more efficiently towards food security.

The rainfall trend analysis of this study clearly shows a significant increase in annual rainfall at the national level from 1983 to 2020 in almost all regions, except the southern and eastern regions. On the other hand, the analysis of the rainfall trend at the regional level has identified an increasing trend in all regions, which can be cited as having a positive impact on agriculture. Furthermore, the study has revealed that countries in the climate zones of Tropical northern desert, Tropical northern semi-arid, and tropical grasslands, where there is the majority of rain-fed agriculture, show a significantly increasing trend in rainfall over all periods of the month, season, and year. Therefore, the increase in rainfall will positively affect the countries' food insecurity in those climate zones. Moreover, another important finding is that the Sahel region is showing an increase in rainfall, despite the severe drought in the recent past of the region. Since a large percentage of Africa's agriculture are rain-dependent, the increasing rainfall trend has a positive effect on climate resilience and adaptation in those areas.

It is important to realize that the southern parts of the Eastern and Southern African regions show trends opposite to those of northern and central Africa. In particular, many of the timeframes considered for this study and the analysis of all geographical units show decreasing rainfall trends. In contrast, the occurrence of frequent flooding in Central African countries may become greater than in the Eastern and Southern African regions, as annual rainfall increases in all the timeframes. Given this, it should be noted that increased rainfall could also hurt food security and climate change tolerance efforts. Despite the increase in rainfall in Western African countries, it is not significant there as it is in other regions.

The findings of this study may help different sectors, such as agriculture, disaster risk reduction, biodiversity conservation, infrastructure development, and climate resilience to enhance respective activities towards the wellbeing of humans and the environment. Furthermore, they are also useful for policy-makers and decision-makers in determining the implications of respective climate adaptation policies. It is recommended to perform country-level comprehensive analysis on flood and drought occurrences to enhance relevant policies in respective countries that indicate increasing or decreasing rainfall trends. Changes in rainfall trends across the African continent identified in this study might be due to changes in long-term atmospheric circulation and monsoon patterns. Thus, it is recommended to conduct a detailed study to explore courses on changes in the rainfall trends.

Author Contributions: Conceptualization, N.A., M.E. and M.R.; Data curation, N.A.; Formal analysis, N.A. and M.E.; Investigation, N.A. and M.E.; Methodology, N.A., M.E., E.P. and M.R.; Resources, N.A.; Supervision, M.E.; Validation, N.A.; Visualization, N.A., M.E., E.P. and M.R.; Writing—original draft, N.A.; Writing—review and editing, N.A., M.E., M.S., V.R.N., E.P. and M.R. All authors have read and agreed to the published version of the manuscript.

Funding: This research received no external funding.

Institutional Review Board Statement: Not applicable.

Informed Consent Statement: Not applicable.

Data Availability Statement: The gridded TAMSAT rainfall products were downloaded from the University of Reading (https://www.tamsat.org.uk/data, accessed on 2 February 2021). African country and region boundaries were downloaded from the World Bank official boundary data catalogue (https://datacatalog.worldbank.org/dataset/world-bank-official-boundaries, accessed on 2 April 2021). The major river basins boundaries were downloaded from the FAO data catalogue (https://data.apps.fao.org/map/catalog/, accessed on 16 April 2021). The climate zone of Africa was generated using a raster dataset (https://www.britannica.com/place/Africa/Climate, accessed on 16 April 2021).

Acknowledgments: The authors are thankful to the TAMSAT Groups as well as the World Bank and FAO for providing the long-term rainfall data, and official boundaries, respectively. Assistance and facilities provided by the International Water Management Institute and Department of Physics, University of Colombo are highly acknowledged. We would like to acknowledge the anonymous reviewers for their valuable suggestions that have helped to improve the manuscript.

Conflicts of Interest: The authors declare no conflict of interest.

Appendix A

Table A1. Descriptive statistics for annual rainfall (in mm) for countries from TAMSAT data (1983 to 2020).

Country	Average	Max	Min	STD	CV	Median
Algeria	121.3	186.6	75.5	23.0	19.0	120.1
Angola	1026.4	1253.6	826.4	106.8	10.4	1017.5
Benin	1083.2	1266.7	736.7	104.9	9.7	1076.7
Botswana	371.2	657.1	198.9	115.8	31.2	345.8
Burkina Faso	739.4	852.7	581.6	52.4	7.1	731.6
Burundi	968.6	1263.7	700.2	148.6	15.3	955.0
Cameroon	1670.3	1909.1	1193.0	153.7	9.2	1708.2
Central African Republic **	1439.9	1721.6	1036.2	167.6	11.6	1486.0
Chad	309.9	386.1	206.6	40.7	13.1	315.6
Congo	1665.5	2074.5	1141.3	189.4	11.4	1663.7
Côte d'Ivoire	1276.4	1538.0	834.7	152.4	11.9	1263.2
Democratic Republic of the Congo ***	1611.2	1807.3	1266.1	130.8	8.1	1644.2
Egypt	39.1	74.2	22.5	12.1	31.0	37.7
Equatorial Guinea	2223.5	2700.6	1420.4	309.3	13.9	2271.2
Eritrea	326.7	443.1	188.3	54.2	16.6	329.3
Ethiopia	816.1	1088.3	561.4	111.1	13.6	816.7
Gabon	1825.4	2312.9	1169.1	254.3	13.9	1899.4
Gambia	770.6	921.0	580.4	80.3	10.4	773.7
Ghana	1195.4	1413.8	776.2	136.4	11.4	1211.9
Guinea	1706.2	1901.5	1523.0	92.1	5.4	1728.1
Kenya	571.0	1001.9	356.4	152.2	26.7	517.6
Lesotho	702.9	860.3	551.5	81.2	11.5	697.7
Liberia	2381.2	3075.2	1653.8	325.0	13.6	2377.5
Libya	61.9	115.0	29.8	16.0	25.9	62.4
Madagascar	1205.8	1503.8	947.8	132.3	11.0	1195.7
Malawi	939.0	1193.1	699.8	126.4	13.5	946.3

Table A1. *Cont.*

Country	Average	Max	Min	STD	CV	Median
Mali	307.8	371.0	239.8	32.3	10.5	304.4
Mauritania	111.2	166.6	65.2	22.9	20.6	107.9
Morocco	299.9	581.2	157.9	87.3	29.1	299.0
Mozambique	807.6	1076.7	577.0	121.5	15.1	808.2
Namibia	243.9	497.7	122.3	86.6	35.5	234.9
Niger	141.5	177.7	79.9	23.2	16.4	143.7
Nigeria	1189.5	1338.0	865.7	84.4	7.1	1196.0
Rwanda	909.3	1248.6	554.2	174.8	19.2	923.1
Senegal	607.3	728.9	456.2	61.3	10.1	606.2
Sierra Leone	2561.0	2841.0	2214.5	175.8	6.9	2556.4
Somalia	311.2	690.7	172.6	109.2	35.1	291.3
South Africa	415.4	517.9	317.4	45.6	11.0	415.9
South Sudan	1011.3	1146.1	842.8	82.0	8.1	1013.3
Sudan	237.6	293.4	138.3	33.7	14.2	242.3
Swaziland	712.4	1065.7	408.9	130.6	18.3	719.1
Togo	1213.2	1414.9	813.1	122.3	10.1	1222.7
Tunisia	255.0	328.8	178.1	37.2	14.6	252.1
Uganda	1262.5	1531.1	980.0	148.6	11.8	1254.5
United Republic of Tanzania *	872.3	1218.6	671.7	132.4	15.2	858.9
Western Sahara	55.1	100.9	18.7	19.3	35.0	55.1
Zambia	981.3	1163.6	742.3	100.9	10.3	992.2
Zimbabwe	601.4	840.6	382.0	120.1	20.0	589.7

* United Republic of Tanzania (URT), ** Central African Republic (CAR), *** Democratic Republic of the Congo (DRC).

Table A2. Descriptive statistics for annual rainfall (in mm) for regions from TAMSAT data (1983 to 2020).

Region	Average	Max	Min	STD	CV	Median
Central	1243.65	1414.44	941.79	111.81	8.99	1258.47
Western	625.89	709.36	464.51	46.27	7.39	626.00
Eastern	786.97	991.73	619.35	86.40	10.98	784.34
Northern	136.06	181.98	83.92	19.34	14.21	137.67
Southern	361.34	539.34	238.74	64.35	17.81	346.92

References

1. IPCC. *Climate Change: The Physical Science Basis*; Solomon, S., Ed.; 2007; p. 1007. Available online: https://www.ipcc.ch/report/ar4/wg1/ (accessed on 10 June 2021).
2. IPCC. *Climate Change: The Physical Science Basis*; Stocker, T.F., Qin, D., Plattner, G.-K., Tignor, M., Allen, S.K., Boschung, J., Nauels, A., Xia, Y., Midgley, P.M., Eds.; Cambridge University Press: Cambridge, UK; New York, NY, USA, 2013; p. 1535. Available online: https://www.ipcc.ch/report/ar5/wg1/ (accessed on 10 June 2021).
3. United Nations International Strategy for Disaster Reduction (UNISDR). *Making Development Sustainable: The Future of Disaster Risk Management*; Global Assessment Report 2015; UN Office for Disaster Risk Reduction: Geneva, Switzerland, 2015.
4. Kotir, J.H. Climate change and variability in Sub-Saharan Africa: A review of current and future trends and impacts on agriculture and food security. *Environ. Dev. Sustain.* **2010**, *13*, 587–605. [CrossRef]
5. Dube, K.; Nhamo, G.; Chikodzi, D. Flooding trends and their impacts on coastal communities of Western Cape Province, South Africa. *GeoJournal* **2021**, 1–16. [CrossRef] [PubMed]
6. Ellwanger, J.H.; Kulmann-Leal, B.; Kaminski, V.L.; Valverde-Villegas, J.M.; Da Veiga, A.B.G.; Spilki, F.R.; Fearnside, P.M.; Caesar, L.; Giatti, L.L.; Wallau, G.L.; et al. Beyond diversity loss and climate change: Impacts of Amazon deforestation on infectious diseases and public health. *An. Acad. Bras. Ciênc.* **2020**, *92*, e20191375. [CrossRef] [PubMed]
7. Dupuy, J.-L.; Fargeon, H.; Martin-StPaul, N.; Pimont, F.; Ruffault, J.; Guijarro, M.; Hernando, C.; Madrigal, J.; Fernandes, P. Climate change impact on future wildfire danger and activity in southern Europe: A review. *Ann. For. Sci.* **2020**, *77*, 35. [CrossRef]
8. Ward, M.; Tulloch, A.I.T.; Radford, J.Q.; Williams, B.A.; Reside, A.E.; Macdonald, S.L.; Mayfield, H.J.; Maron, M.; Possingham, H.P.; Vine, S.J.; et al. Impact of 2019–2020 mega-fires on Australian fauna habitat. *Nat. Ecol. Evol.* **2020**, *4*, 1321–1326. [CrossRef]

9. Libonati, R.; Pereira, J.M.C.; Da Camara, C.C.; Peres, L.F.; Oom, D.; Rodrigues, J.A.; Santos, F.L.M.; Trigo, R.M.; Gouveia, C.M.P.; Machado-Silva, F.; et al. Twenty-first century droughts have not increasingly exacerbated fire season severity in the Brazilian Amazon. *Sci. Rep.* **2021**, *11*, 4400. [CrossRef]
10. Gornall, J.; Betts, R.; Burke, E.; Clark, R.; Camp, J.; Willett, K.; Wiltshire, A. Implications of climate change for agricultural productivity in the early twenty-first century. *Philos. Trans. R. Soc. B Biol. Sci.* **2010**, *365*, 2973–2989. [CrossRef]
11. Hulme, P.E. Adapting to climate change: Is there scope for ecological management in the face of a global threat? *J. Appl. Ecol.* **2005**, *42*, 784–794. [CrossRef]
12. ForestPlots.net; Blundo, C.; Carilla, J.; Grau, R.; Malizia, A.; Malizia, L.; Osinaga-Acosta, O.; Bird, M.; Bradford, M.; Catchpole, D.; et al. Taking the pulse of Earth's tropical forests using networks of highly distributed plots. *Biol. Conserv.* **2021**, *260*, 108849. [CrossRef]
13. Ebhuoma, E.; Simatele, D. Defying the odds: Climate variability, asset adaptation and food security nexus in the Delta State of Nigeria. *Int. J. Disaster Risk Reduct.* **2017**, *21*, 231–242. [CrossRef]
14. Lawrimore, J.H.; Halpert, M.S.; Bell, G.D.; Menne, M.J.; Lyon, B.; Schnell, R.C.; Gleason, K.L.; Easterling, D.R.; Thiaw, W.; Wright, W.J. Climate assessment for 2000. *Bull. Am. Meteorol. Soc.* **2001**, *82*, S1–S62. [CrossRef]
15. New, M.; Todd, M.; Hulme, M.; Jones, P. Precipitation measurements and trends in the twentieth century. *Int. J. Clim.* **2001**, *21*, 1889–1922. [CrossRef]
16. González-Hidalgo, J.C.; Brunetti, M.; de Luis, M. A new tool for monthly precipitation analysis in Spain: MOPREDAS database (monthly precipitation trends December 1945–November 2005). *Int. J. Clim.* **2011**, *31*, 715–731. [CrossRef]
17. Brunetti, M.; Maugeri, M.; Monti, F.; Nanni, T. Temperature and precipitation variability in Italy in the last two centuries from homogenised instrumental time series. *Int. J. Clim.* **2006**, *26*, 345–381. [CrossRef]
18. Norrant, C.; Douguédroit, A. Monthly and daily precipitation trends in the Mediterranean (1950–2000). *Theor. Appl. Clim.* **2005**, *83*, 89–106. [CrossRef]
19. Caloiero, T.; Coscarelli, R.; Ferrari, E.; Mancini, M. Precipitation change in Southern Italy linked to global scale oscillation indexes. *Nat. Hazards Earth Syst. Sci.* **2011**, *11*, 1683–1694. [CrossRef]
20. Gebrechorkos, S.H.; Hülsmann, S.; Bernhofer, C. Long-term trends in rainfall and temperature using high-resolution climate datasets in East Africa. *Sci. Rep.* **2019**, *9*, 11376. [CrossRef]
21. Alahacoon, N.; Edirisinghe, M. Spatial Variability of Rainfall Trends in Sri Lanka from 1989 to 2019 as an Indication of Climate Change. *ISPRS Int. J. Geo-Inf.* **2021**, *10*, 84. [CrossRef]
22. Barrios, S.; Bertinelli, L.; Strobl, E. Trends in Rainfall and Economic Growth in Africa: A Neglected Cause of the African Growth Tragedy. *Rev. Econ. Stat.* **2010**, *92*, 350–366. [CrossRef]
23. FAO. *The State of Food and Agriculture 2014. Innovation in Family Farming*; FAO: Rome, Italy, 2014.
24. Nicholson, S.E. Climate and climatic variability of rainfall over eastern Africa. *Rev. Geophys.* **2017**, *55*, 590–635. [CrossRef]
25. Sidibe, M.; Dieppois, B.; Eden, J.; Mahé, G.; Paturel, J.-E.; Amoussou, E.; Anifowose, B.; Van De Wiel, M.; Lawler, D. Near-term impacts of climate variability and change on hydrological systems in West and Central Africa. *Clim. Dyn.* **2020**, *54*, 2041–2070. [CrossRef]
26. Diba, I.; Camara, M.; Diedhiou, A. Investigating West African Monsoon Features in Warm Years Using the Regional Climate Model RegCM4. *Atmosphere* **2019**, *10*, 23. [CrossRef]
27. Vischel, T.; Panthou, G.; Peyrillé, P.; Roehrig, R.; Quantin, G.; Lebel, T.; Wilcox, C.; Beucher, F.; Budiarti, M. Precipitation extremes in the West African Sahel: Recent evolution and physical mechanisms. In *Tropical Extremes*; Elsevier: Amsterdam, The Netherlands, 2019; pp. 95–138.
28. Biasutti, M. Rainfall trends in the African Sahel: Characteristics, processes, and causes. *Wiley Interdiscip. Rev. Clim. Chang.* **2019**, *10*, 591. [CrossRef]
29. Dosio, A.; Jones, R.G.; Jack, C.; Lennard, C.; Nikulin, G.; Hewitson, B. What can we know about future precipitation in Africa? Robustness, significance and added value of projections from a large ensemble of regional climate models. *Clim. Dyn.* **2019**, *53*, 5833–5858. [CrossRef]
30. Nicholson, S.E.; Klotter, D.A. Assessing the Reliability of Satellite and Reanalysis Estimates of Rainfall in Equatorial Africa. *Remote Sens.* **2021**, *13*, 3609. [CrossRef]
31. Endris, H.S.; Omondi, P.; Jain, S.L.; Lennard, C.; Hewitson, B.; Chang'A, L.; Awange, J.; Dosio, A.; Ketiem, P.; Nikulin, G.; et al. Assessment of the Performance of CORDEX Regional Climate Models in Simulating East African Rainfall. *J. Clim.* **2013**, *26*, 8453–8475. [CrossRef]
32. Endris, H.S.; Lennard, C.; Hewitson, B.; Dosio, A.; Nikulin, G.; Panitz, H.-J. Teleconnection responses in multi-GCM driven CORDEX RCMs over Eastern Africa. *Clim. Dyn.* **2016**, *46*, 2821–2846. [CrossRef]
33. Fer, I.; Tietjen, B.; Jeltsch, F.; Wolff, C. The influence of El Niño–Southern Oscillation regimes on eastern African vegetation and its future implications under the RCP8.5 warming scenario. *Biogeosciences* **2017**, *14*, 4355–4374. [CrossRef]
34. Mpelasoka, F.; Awange, J.L.; Zerihun, A. Influence of coupled ocean-atmosphere phenomena on the Greater Horn of Africa droughts and their implications. *Sci. Total Environ.* **2018**, *610–611*, 691–702. [CrossRef]
35. Lei, Y.; Hoskins, B.; Slingo, J. Exploring the Interplay between Natural Decadal Variability and Anthropogenic Climate Change in Summer Rainfall over China. Part I: Observational Evidence. *J. Clim.* **2011**, *24*, 4584–4599. [CrossRef]

36. Mahmud, M.R.; Numata, S.; Matsuyama, H.; Hosaka, T.; Hashim, M. Challenge and opportunities of space-based precipitation radar for spatio-temporal hydrology analysis in tropical maritime influenced catchment: Case study on the hilly tropical watershed of Peninsular Malaysia. In Proceedings of the IOP Conference Series: Earth and Environmental Science, Kuching, Malaysia, 26–29 August 2013; IOP Publishing: Bristol, UK, 2014; Volume 18, p. 12001.
37. Niang, I.; Ruppel, O.C.; Abdrabo, M.A.; Essel, A.; Lennard, C.; Padgham, J.; Urquhart, P. Africa. In Climate Change 2014: Impacts, Adaptation, and Vulnerability. Part B: Regional Aspects. Contribution of Working Group II to the Fifth Assessment Report of the Intergovernmental Panel on Climate Change. 2014. Available online: https://www.ipcc.ch/site/assets/uploads/2018/02/WGIIAR5-Chap22_FINAL.pdf (accessed on 15 May 2021).
38. Washington, R.; Harrison, M.; Conway, D.; Black, E.; Challinor, A.; Grimes, D.; Jones, R.; Morse, A.; Kay, G.; Todd, M. African Climate Change: Taking the Shorter Route. *Bull. Am. Meteorol. Soc.* **2006**, *87*, 1355–1366. [CrossRef]
39. Wodon, Q.; Liverani, A.; Joseph, G.; Bougnoux, N. (Eds.) *Climate Change and Migration: Evidence from the Middle East and North Africa*; World Bank Publications: Washington, DC, USA, 2014. [CrossRef]
40. Liebmann, B.; Hoerling, M.P.; Funk, C.; Bladé, I.; Dole, R.M.; Allured, D.; Quan, X.; Pegion, P.; Eischeid, J.K. Understanding Recent Eastern Horn of Africa Rainfall Variability and Change. *J. Clim.* **2014**, *27*, 8630–8645. [CrossRef]
41. Yang, W.; Seager, R.; Cane, M.A.; Lyon, B. The East African Long Rains in Observations and Models. *J. Clim.* **2014**, *27*, 7185–7202. [CrossRef]
42. Maidment, R.; Grimes, D.; Black, E.; Tarnavsky, E.; Young, M.; Greatrex, H.; Allan, R.; Stein, T.; Nkonde, E.; Senkunda, S.; et al. Erratum: A new, long-term daily satellite-based rainfall dataset for operational monitoring in Africa. *Sci. Data* **2017**, *4*, 170063. [CrossRef]
43. Cattani, E.; Merino, A.; Guijarro, J.A.; Levizzani, V. East Africa Rainfall Trends and Variability 1983–2015 Using Three Long-Term Satellite Products. *Remote Sens.* **2018**, *10*, 931. [CrossRef]
44. Tarnavsky, E.; Grimes, D.; Maidment, R.; Black, E.; Allan, R.; Stringer, M.; Chadwick, R.; Kayitakire, F. Extension of the TAMSAT Satellite-Based Rainfall Monitoring over Africa and from 1983 to Present. *J. Appl. Meteorol. Clim.* **2014**, *53*, 2805–2822. [CrossRef]
45. Thiemig, V.; Rojas, R.; Zambrano-Bigiarini, M.; Levizzani, V.; De Roo, A. Validation of Satellite-Based Precipitation Products over Sparsely Gauged African River Basins. *J. Hydrometeorol.* **2012**, *13*, 1760–1783. [CrossRef]
46. Maidment, R.I.; Grimes, D.I.F.; Allan, R.; Greatrex, H.; Rojas, O.; Leo, O. Evaluation of satellite-based and model re-analysis rainfall estimates for Uganda. *Meteorol. Appl.* **2012**, *20*, 308–317. [CrossRef]
47. Pfeifroth, U.; Trentmann, J.; Fink, A.H.; Ahrens, B. Evaluating Satellite-Based Diurnal Cycles of Precipitation in the African Tropics. *J. Appl. Meteorol. Clim.* **2016**, *55*, 23–39. [CrossRef]
48. Toté, C.; Patricio, D.; Boogaard, H.; Van Der Wijngaart, R.; Tarnavsky, E.; Funk, C. Evaluation of Satellite Rainfall Estimates for Drought and Flood Monitoring in Mozambique. *Remote Sens.* **2015**, *7*, 1758–1776. [CrossRef]
49. Simpson, J.; Adler, R.F.; North, G.R. A Proposed Tropical Rainfall Measuring Mission (TRMM) Satellite. *Bull. Am. Meteorol. Soc.* **1988**, *69*, 278–295. [CrossRef]
50. Arkin, P.A.; Xie, P. The Global Precipitation Climatology Project: First Algorithm Intercomparison Project. *Bull. Am. Meteorol. Soc.* **1994**, *75*, 401–419. [CrossRef]
51. Yatagai, A.; Arakawa, O.; Kamiguchi, K.; Kawamoto, H.; Nodzu, M.I.; Hamada, A. A 44-Year Daily Gridded Precipitation Dataset for Asia Based on a Dense Network of Rain Gauges. *Sola* **2009**, *5*, 137–140. [CrossRef]
52. Hou, A.Y.; Kakar, R.K.; Neeck, S.; Azarbarzin, A.A.; Kummerow, C.D.; Kojima, M.; Oki, R.; Nakamura, K.; Iguchi, T. The global precipitation measurement mission. *Bull. Am. Meteorol. Soc.* **2014**, *95*, 701–722. [CrossRef]
53. Hsu, K.-L.; Gao, X.; Sorooshian, S.; Gupta, H.V. Precipitation Estimation from Remotely Sensed Information Using Artificial Neural Networks. *J. Appl. Meteorol.* **1997**, *36*, 1176–1190. [CrossRef]
54. Funk, C.; Peterson, P.; Landsfeld, M.; Pedreros, D.; Verdin, J.; Shukla, S.; Husak, G.; Rowland, J.; Harrison, L.; Hoell, A.; et al. The climate hazards infrared precipitation with stations—A new environmental record for monitoring extremes. *Sci. Data* **2015**, *2*, 150066. [CrossRef]
55. Kinda, S.R.; Badolo, F. Does rainfall variability matter for food security in developing countries? *Cogent Econ. Financ.* **2019**, *7*, 1640098. [CrossRef]
56. Rockström, J.; Barron, J.; Fox, P. Water productivity in rain-fed agriculture: Challenges and opportunities for smallholder farmers in drought-prone tropical agroecosystems. In *Water Productivity in Agriculture: Limits and Opportunities for Improvement*; CABI Publishing: Wallingford, UK, 2009; pp. 145–162.
57. FAO; IFAD; WFP. *The State of Food Insecurity in the World 2014. Strengthening the Enabling Environment for Food Security and Nutrition*; FAO: Rome, Italy, 2014; Available online: https://www.fao.org/3/i4030e/i4030e.pdf (accessed on 18 June 2021).
58. Wani, S.P.; Rockström, J.; Oweis, T.Y. (Eds.) *Rainfed Agriculture: Unlocking the Potential*; CABI: Wallingford, UK, 2009; Volume 7. Available online: http://www.iwmi.cgiar.org/Publications/CABI_Publications/CA_CABI_Series/Rainfed_Agriculture/Protected/Rainfed_Agriculture_Unlocking_the_Potential.pdf (accessed on 10 June 2021).
59. Kyei-Mensah, C.; Kyerematen, R.; Adu-Acheampong, S. Impact of Rainfall Variability on Crop Production within the Worobong Ecological Area of Fanteakwa District, Ghana. *Adv. Agric.* **2019**, *2019*, 7930127. [CrossRef]
60. Adeyewa, Z.D.; Nakamura, K. Validation of TRMM radar rainfall data over major climatic regions in Africa. *J. Appl. Meteorol.* **2003**, *42*, 331–347. [CrossRef]

61. Dubois, O. *The State of the World's Land and Water Resources for Food and Agriculture: Managing Systems at Risk*; Earthscan: London, UK, 2011. Available online: https://www.fao.org/3/i1688e/i1688e01.pdf (accessed on 11 May 2021).
62. Qian, H.; Zhou, Y.; Zhang, J.; Jin, Y.; Deng, T.; Cheng, S. A synthesis of botanical informatics for vascular plants in Africa. *Ecol. Inform.* **2021**, *64*, 101382. [CrossRef]
63. Mendelson, M.; Han, P.V.; Vincent, P.; Von Sonnenburg, F.; Cramer, J.P.; Loutan, L.; Kain, K.; Parola, P.; Hagmann, S.; Gkrania-Klotsas, E.; et al. Regional Variation in Travel-related Illness acquired in Africa, March 1997–May 2011. *Emerg. Infect. Dis.* **2014**, *20*, 532–541. [CrossRef]
64. Arsenault, K.R.; Shukla, S.; Getirana, A.; Peters-Lidard, C.D.; Kumar, S.; McNally, A.; Zaitchik, B.F.; Badr, H.S.; Funk, C.C.; Koster, R.D.; et al. Using Satellite Data and Land Surface Models to Monitor and Forecast Drought Conditions in Africa and Middle East. In *AGU Fall Meeting Abstracts (Vol. 2017, H22F-05)*. Available online: https://ui.adsabs.harvard.edu/abs/2017AGUFM.H22F..05A/abstract (accessed on 14 July 2021).
65. Asfaw, D.; Black, E.; Brown, M.; Nicklin, K.J.; Otu-Larbi, F.; Pinnington, E.; Challinor, A.; Maidment, R.; Quaife, T. TAMSAT-ALERT v1: A new framework for agricultural decision support. *Geosci. Model Dev.* **2018**, *11*, 2353–2371. [CrossRef]
66. Seyama, E.S.; Masocha, M.; Dube, T. Evaluation of TAMSAT satellite rainfall estimates for southern Africa: A comparative approach. *Phys. Chem. Earth Parts A/B/C* **2019**, *112*, 141–153. [CrossRef]
67. Grimes, D.; Pardo-Igúzquiza, E.; Bonifacio, R. Optimal areal rainfall estimation using raingauges and satellite data. *J. Hydrol.* **1999**, *222*, 93–108. [CrossRef]
68. Wang, W.; Chen, X.; Shi, P.; Van Gelder, P.H.A.J.M.; Corzo, G. Extreme precipitation and extreme streamflow in the Dongjiang River Basin in southern China. *Hydrol. Earth Syst. Sci. Discuss.* **2007**, *4*, 2323–2360.
69. Pal, A.B.; Khare, D.; Mishra, P.K.; Singh, L. Trend Analysis of Rainfall, Temperature and Runoff Data: A Case Study of Rangoon Watershed in Nepal. *Int. J. Stud. Res. Technol. Manag.* **2017**, *5*, 21–38. [CrossRef]
70. Ali, R.; Kuriqi, A.; Abubaker, S.; Kisi, O. Long-Term Trends and Seasonality Detection of the Observed Flow in Yangtze River Using Mann-Kendall and Sen's Innovative Trend Method. *Water* **2019**, *11*, 1855. [CrossRef]
71. Kendall, M.G. *Rank Correlation Methods*; Charles Griffin & Co.: London, UK, 1948.
72. Gadgil, A.; Dhorde, A. Temperature trends in twentieth century at Pune, India. *Atmos. Environ.* **2005**, *39*, 6550–6556. [CrossRef]
73. Sen, P.K. Estimates of the regression coefficient based on Kendall's Tau. *J. Am. Stat. Assoc.* **1968**, *63*, 1379–1389. [CrossRef]
74. Beck, H.E.; Zimmermann, N.E.; McVicar, T.R.; Vergopolan, N.; Berg, A.; Wood, E.F. Present and future Köppen-Geiger climate classification maps at 1-km resolution. *Sci. Data* **2018**, *5*, 180214. [CrossRef]
75. Peterson, T.C.; Stott, P.; Herring, S. Explaining Extreme Events of 2011 from a Climate Perspective. *Bull. Am. Meteorol. Soc.* **2012**, *93*, 1041–1067. [CrossRef]
76. Williams, A.P.; Funk, C.C.; Michaelsen, J.; Rauscher, S.A.; Robertson, I.; Wils, T.H.G.; Koprowski, M.; Eshetu, Z.; Loader, N.J. Recent summer precipitation trends in the Greater Horn of Africa and the emerging role of Indian Ocean sea surface temperature. *Clim. Dyn.* **2012**, *39*, 2307–2328. [CrossRef]
77. Gebrechorkos, S.H.; Hülsmann, S.; Bernhofer, C. Evaluation of multiple climate data sources for managing environmental resources in East Africa. *Hydrol. Earth Syst. Sci.* **2018**, *22*, 4547–4564. [CrossRef]
78. Nouaceur, Z.; Murarescu, O. Rainfall Variability and Trend Analysis of Annual Rainfall in North Africa. *Int. J. Atmos. Sci.* **2016**, *2016*, 7230450. [CrossRef]